Characterizing the Brain Tumor Microenvironment

Heather Anderson-Keightly

Integrated Program in Neuroscience (IPN)
McGill University, Montreal

June 2019

A thesis submitted to McGill University in partial fulfillment of the requirements of the degree of Master's in Science.

© Heather Anderson-Keightly 2019

Table of Contents

List of Figures

Abstract

Background: Targeting the tumor microenvironment has become a promising avenue of oncology, however little is known about this aspect in medulloblastoma. The tumor microenvironment includes many components which may either inhibit or promote malignant growth. Tumor-associated macrophages (TAMs) and neutrophils have demonstrated both pro- and anti-tumoral activity that can vary between tumor types. Senescent cells exhibit a senescent associated secretory phenotype (SASP) which can affect neighboring tumor cells, immune cell infiltration, and cell differentiation. We aimed to characterize the tumor microenvironment in the pediatric brain tumor Sonic Hedgehog (Shh) medulloblastoma.

Methods/Results: Using the Ptch1$^{+/-}$ mouse model of Shh medulloblastoma, we have shown that the tumor microenvironment evolves as the tumor develops. In preneoplasia there are macrophages and senescent cells. Peripheral macrophage depletion with clodronate liposomes did not affect TAM density early in tumorigenesis, suggesting that at the preneoplastic stage TAMs originate from the microglia rather than the periphery. Through ablation with Navitoclax, we found that senescent cells restrict preneoplasia growth. Advanced tumors have a more complex microenvironment including macrophages and neutrophils. Both M1-like and M2-like macrophages are present in tumors, and they aggregate in regions of high apoptosis and low proliferation. Through comparing tissues of bypassed senescence or potentially-unrestricted SASP activity, we show that neither macrophage, neutrophil, nor stem cell densities are affected by senescent cells.

Conclusion: Our results demonstrate that the tumor microenvironment of medulloblastoma evolves, becoming more complex as the tumor progresses to advanced stage. Senescent cells restrict tumor growth during early stages, suggesting their SASP is inducing paracrine senescence. Understanding the tumor microenvironment of medulloblastoma may lend insights into how this tumor can be targeted with immunotherapy agents.

Résumé

Contexte: Le microenvironnement tumoral est devenu une avenue prometteuse en oncologie, mais on en sait peu sur cet aspect dans le médulloblastome. Le microenvironnement de la tumeur comprend de nombreux composants qui peuvent inhiber ou encourager la croissance maligne. Les macrophages associés aux tumeurs (TAM) et les neutrophiles ont démontré une activité à la fois pro- et antitumorale pouvant varier d'un type de tumeur à l'autre. Les cellules sénescentes présentent un phénotype de sécrétion associé à la sénescence (SASP) pouvant affecter les cellules tumorales voisines, l'infiltration de cellules immunitaires et la différenciation cellulaire. Notre objectif était de caractériser le microenvironnement tumoral dans le médulloblastome Sonic Hedgehog (Shh).

Méthodes / Résultats: En utilisant le modèle murin Ptch1 +/- du médulloblastome de Shh, nous avons montré que le microenvironnement tumoral évoluait en même temps que la tumeur. Dans la prénéoplasie, il existe des macrophages et des cellules sénescentes. L'épuisement des macrophages périphériques avec les liposomes de clodronate n'a pas affecté la densité de TAM au début de la tumorigenèse, ce qui suggère que les TAM au stade prénéoplasique proviennent de la microglie plutôt que de la périphérie. Grâce à l'ablation avec Navitoclax, nous avons constaté que les cellules sénescentes limitent la croissance de la prénéoplasie. Les tumeurs avancées ont un microenvironnement plus complexe comprenant des macrophages et des neutrophiles. Les macrophages de type M1 et de type M2 sont présents dans les tumeurs et s'agrègent dans les régions à forte apoptose et à faible prolifération. En comparant les tissus de sénescence contournée ou d'activité SASP potentiellement non restreinte, nous montrons que ni les cellules infiltrées par les macrophages ni les neutrophiles ne sont affectées par les cellules sénescentes.

Conclusion: Nos résultats démontrent que le microenvironnement tumoral du médulloblastome évolue, devenant de plus en plus complexe à mesure que la tumeur progresse au stade avancé. Les cellules sénescentes limitent la croissance tumorale au cours des stades précoces, ce qui suggère que leur SASP induit une sénescence paracrine. Comprendre le microenvironnement tumoral du médulloblastome peut aider à comprendre comment cette tumeur peut être ciblée avec des agents d'immunothérapie.

Acknowledgements

Throughout my Master's degree I have had the pleasure to meet many outstanding and supportive people that were instrumental to my professional and personal development.

First, I would like to thank my supervisor Dr. Frédéric Charron for accepting me into his lab, for his mentorship and help on the project, and for fostering a positive lab environment. I want to thank the current and past members of the lab who made coming to work a joy every day: Nursen Balekoglu, Dr. Sara Calabretta, Dr. Francois Depault, Dr. Julien Ferent, Dr. Shirin Makihara, Jean-Francois Michaud, Sushmetha Mohan, Dr. Frédéric Racicot, Dr. Sabrina Schlienger, Shannon Swikert, Dr. Lukas Tamayo-Orrego, Dr. Chia-Lun Wu, and Dr. Patricia Yam. Lukas, Sabrina, Shannon, and Chia-Lun taught me lab techniques and were always willing to discuss my project to troubleshoot issues. More than just co-workers, the members of the lab also became my close friends. Exploring Montreal, lab 5á7s, going to the Opera and Cinema, camping trips, trying new restaurants and bars, and sharing our diverse cultures are just a few of the fun things we did together. I also extend a special thanks to Sabrina, Julien, and Shannon who supported me in various ways during difficult times in my personal life. I feel honored and grateful to have made such wonderful friends, and they truly feel like my "family away from family." While I'm sad we are all going to different cities, I am excited for the network we form around the world because it means I get to visit fun places!

I would like to thank my committee members, Dr. Francis Rodier and Dr. David Dankort, for their time, support, and suggestions for the project; Dr. Heather Durham, my IPN mentor, for her time and support; and Dr. Dusica Maysinger for attending my MSc Thesis Seminar.

I would like to thank members of the IRCM: Dominic Fillion for microscopy instruction; Marie-Anne Riquelme Jacob, Sara Demontigny, Manon Laprise, Caroline Dube, Valerie Darisse-Lafrance, Yesenia Alvis, and Jessica Barthe for their work in the animal care facility and boundless patience with my constant requests. I also thank Michel Fries for teaching me MEF isolation; as well as members of the Cayoutte, Kania, and Takahashi labs for their suggestions on my project during Neuroclub meetings, and friendships. I am also thankful to the Veillette and Suh labs who generously allowed us to borrow antibodies.

I am very thankful for the funding from the Michel-F-Belanger family, whose fellowship the IRCM awarded me two years in a row, and for the Healthy Brains for Healthy Lives Master's Scholarship from McGill University.

I would like to thank Dr. Alexander Jaworski, who continued to make time to mentor me even though I'm no longer in his lab, and always answered my emails in record-breaking time.

Lastly I would like to thank my family who supported me when I faced adversity and felt discouraged: my grandmother, Corinne Keightly, who was my biggest cheerleader, my aunt, Amy Tomalin, who constantly encourages me to "grab the bull by the horns!," as well as my parents, David Keightly and Jill Anderson. Thank you!

Preface and Contribution of Authors

This thesis was written in accordance with McGill University's "Guidelines for Thesis Preparation." The data presented in this thesis is mainly the original work of the candidate.

1. Heather Anderson-Keightly (HAK) and Frederic Charron (FC) designed the research;
2. HAK, Marie-Anne Riquelme Jacob (MARJ), Chia-Lun Wu (CLW), Lukas Tamayo-Orrego (LTO), and Sabrina Schlienger (SS) performed the following research:
    a. MARJ helped with oral gavage of ABT263
    b. CLW generated the in-utero electroporation tumors using CRISPR-Ptch1 and CRISPR-Ptch1-p16
    c. LTO collected and genotyped the p53 wild type and mutant tumors from Ptch1 mice
    d. SS helped with isolation of granule cell precursors and use of siRNA and CRISPR-Cas9 against Ptch1
    e. HAK performed the rest of the experiments

List of Abbreviations

BMDM	bone marrow derived macrophages
EGL	external granule layer (cerebellum)
GCPs	granule cell precursors
GEMMS	genetically engineered mouse model
gMDSC	granulocytic myeloid derived suppressor cell
IF	immunofluorescence
IHC	immunohistochemistry
MDSC	myeloid derived suppressor cell
MEFs	mouse embryonic fibroblasts
mMDSC	monocytic myeloid derived suppressor cell
NK cells	natural killer cells
P#	postnatal day #
SA-Bgal	senescence associated beta-galactosidase
SASP	senescence-associated secretory phenotype
SHH/Shh	sonic hedgehog
SMO	smoothened
TAMs	tumor-associated macrophages

Introduction

Tumor Microenvironment

At the turn of the 21st century, Hanahan and Weinberg released a seminal paper on the "hallmarks of cancer," illustrating the traits acquired by neoplastic cells across all malignancies (Hanahan & Weinberg, 2000). In 2011, they updated their paradigm with an emphasis on the tumor microenvironment, adding several new "emerging and enabling" hallmarks such as tumor-promoting inflammation. Historically, tumor-associated inflammation was believed to be a part of the body's fight against cancer, yet surprising evidence of inflammation fostering neoplasm through supply of bioactive molecules and secretion of factors stimulating angiogenesis, growth, invasiveness, and survival has challenged this dogma (Hanahan & Weinberg, 2011). Thus, the tumor microenvironment has gained recent attention; specifically, how this "soil" creates a niche for tumor growth, how it changes as a tumor evolves, if it may predict prognosis, and if it can be exploited to fight cancer. The tumor microenvironment is comprised of several diverse components, including stromal cells, extracellular matrix, blood vessels, fibroblasts, cancer stem cells, senescent cells, immune cells, and more (Hanahan & Weinberg, 2011; Wang et al., 2017).

Immune cell infiltration of variable levels has been described in nearly all malignancies. Both leukocytes of adaptive and innate immunity have been associated with the tumor microenvironment, including B cells, T cells, macrophages, natural killer (NK) cells, dendritic cells, and small granulocytes such as neutrophils and eosinophils (Wang et al., 2017). To investigate the prognostic significance of these cell types, one study analyzed the relationship between leukocyte infiltration signatures and overall survival using 5,782 tumors from 25 different types of cancer. The cells that significantly correlated with favorable prognosis were a subset of T

cells, meanwhile the cells that associated with adverse prognosis were macrophages and small granulocytes (Gentles et al., 2015).

Of immune cell infiltrates, tumor-associated macrophages (TAMs) may be the most well-characterized. A rigorous meta-analysis in 2012 of 55 studies (n=8,692) revealed that high TAM density was associated with late clinical staging and/or poor overall survival in several types of cancers including gastric, breast, bladder, ovarian, oral, and thyroid (Zhang et al., 2012). This is not consistent across all tumors though, such as in colorectal cancer, where high TAM density correlates with increased overall survival (Forssell et al., 2007; Zhang et al., 2012).

Functional studies in mouse models further support the pro-tumoral activity of TAMs. Macrophage depletion mediated by clodronate liposomes reduced tumor growth in several tumor types (reviewed in (Qian & Pollard, 2010)). Additionally, inhibition of cytokines associated with TAM recruitment, such as CCL2 and CSF1, demonstrated decrease tumor growth in several cancers (DeNardo et al., 2011; Pyonteck et al., 2013; Qian et al., 2011; Ries et al., 2014). Yet just as with the clinical data, there are conflicting results in the literature. For example, while liver-specific macrophages, Kupffer cells, were believed to be tumor-promoting through NFκB signaling, Kupffer cell depletion studies in mice and rats led to increased metastasis formation (Qian & Pollard, 2010).

Macrophage heterogeneity may be a source of these conflicting results. Historically, macrophages were described based on two polarized states: M1 which are classically active, phagocytic, and pro-inflammatory, and M2, which are alternatively active and pro-tissue repair. While these definitions are an oversimplification of the complex activity of highly plastic cells, they are still often used due to absence of a more relevant classification (Murray et al., 2014). Studies have shown both M1-like and M2-like TAMs, with the former associated with anti-tumoral

activity, and the later associated with pro-tumoral activity. Tumor-promoting M2-like TAMs secrete a variety of factors that can induce proliferation, angiogenesis, metastasis, and adaptive immunity suppression (for more review on M2-like TAMs see (Mantovani, Sozzani, Locati, Allavena, & Sica, 2002; Rhee, 2016)). In addition to secretion of cytokines and growth factors, M2-like macrophages may also transfer cytoplasm to tumor cells through direct contact, promoting tumor cell dissemination, as demonstrated in a zebrafish melanoma model (Roh-Johnson et al., 2017). Some studies have suggested updated TAM classifications based on activity and locations in the tumors, such as: metastatic, invasive, angiogenic, perivascular, border-associated, and hypoxia-entrained (Lewis, Harney, & Pollard, 2016; Mehrabi, Amini, & Mehrabi, 2018; Qian & Pollard, 2010).

The driver of TAM heterogeneity is not fully understood, but one contributing factor may be ontology. Many solid-tumors are located in organs that contain a population of tissue-resident macrophages. Thus TAMs in those tumors may originate from the circulation or *in situ*. Investigating TAM ontology can be difficult due to macrophage plasticity; circulating macrophages can adopt a similar transcriptional profile to tissue-resident macrophage upon infiltration (Quail & Joyce, 2017; Scott et al., 2016). However, through genetically modified mouse models (GEMMs), bone-marrow transplant and parabiosis experiments, *Franklin et al., 2014* showed that majority of the TAM population in breast tumors is derived from CCR-expressing circulating monocytes, not macrophages resident of the breast. Depletion of those circulating monocytes resulted in reduced tumor burden (Franklin et al., 2014). Similarly, CCR-CCL inhibition in a metastatic model of breast cancer led to decreased TAM infiltration and consequently reduced metastasis (Qian et al., 2011). Depletion of macrophages using clodronate liposomes has shown reduced tumor growth in models of melanoma, ovarian, lewis lung,

teratocarcinoma, rhabdomyosarcoma, and prostate tumor graph models (for full review see (Qian & Pollard, 2010)). Together these results suggest that TAMs derived from circulating monocytes have tumor-promoting activity. Yet not all studies support this claim. Using parabiosis, bone marrow transplant, and GEMMs, a 2017 study demonstrated that circulating monocytes comprised only ~30% of the TAM population in pancreatic adenocarcinoma. Only depletion of pancreas-resident macrophages, not circulating monocytes, led to decreased tumor burden (Y. Zhu et al., 2017). This suggests that ontology and tumor type may affect TAM activity, and it should not be assumed that all TAMs will have the same effect on tumor growth.

Ontology alone does not dictate a macrophage's activity, which may switch from activated, anti-inflammatory during early stages of tumorigenesis, to trophic, tumor-promoting during later stages (Cassetta & Kitamura, 2018; Qian & Pollard, 2010). Hypoxia is one aspect of the tumor microenvironment which may alter macrophage activity. Hypoxic regions are necrosis-rich areas associated with aggregates of M2-like macrophages that promote tumor regrowth (Chen et al., 2009; Mehrabi et al., 2018). Signals secreted by hypoxic cells such as CCL2, CCL5, and VEGF recruit macrophages which can become desensitized from the onslaught of debris, leading to upregulation of regenerative and immunosuppressive genes (Mehrabi et al., 2018). Those macrophages may also become senescent, leading to an accumulation of non-functional cells that increase tumor inflammation (Mehrabi et al., 2018).

Another class of suspected tumor-promoting cells are myeloid-derived suppressor cells (MDSC). These are immature cells that can be monocytic (mMDSC), resembling TAMs, or granulocytic (gMDSC), resembling neutrophils. MDSCs are recruited to tumors through cytokines CCL2, CXCL12, and CXCL5, and exert a pro-tumorigenic effect on neighboring cells through secretion of Arg1 and iNOS, as well as stimulating angiogenesis (Murdoch, Muthana, Coffelt, &

Lewis, 2008). Hypoxic regions of tumors can attract MDSCs and upregulate immunosuppressive ligands on their surface, such as PD-L1 (Kumar, Patel, Tcyganov, & Gabrilovich, 2016). Depletion of MDSCs in colorectal, lung, and metastatic breast tumor models displayed reduced angiogenesis and decreased tumor burden (summarized in (Murdoch et al., 2008)). MDSCs should be identified primarily through their immunosuppressive activity rather than cell surface markers, as mMDSCs and gMDSCs often express the same markers as TAMs and neutrophils, respectively (Kumar et al., 2016). For that reason, one cannot distinguish between neutrophils and MDSCs from expression of Gr1 or Ly6G/Ly6C alone, complexifying the evidence in the literature regarding neutrophil involvement in tumorigenesis.

Neutrophils are abundant, small granulocytes whose role in tumorigenesis is ambiguous. On one hand, neutrophils have anti-tumor activity, including recruitment of additional phagocytic cells, promotion of T cell-mediated immunity, and detachment of cancer cells to the basement membrane (Powell & Huttenlocher, 2016). This has been confirmed in functional studies, which showed blockage of MMP9, G-CSFR and CXCR2, and MET-mediated neutrophil infiltration increased tumor burden in breast, uterine, and liver cancer mouse models, respectively (Blaisdell et al., 2015; Finisguerra et al., 2015; Leifler et al., 2013). However, neutrophil infiltration is associated with increasing grade in gliomas and poor clinical outcome in certain forms of uterine, lung, liver, colorectal, head and neck, brain, and pancreatic cancers (Fossati et al., 1999; Galdiero et al., 2013). In fact, neutrophil to lymphocyte ratio is proposed as a potential biomarker for patient stratification (Coffelt, Wellenstein, & de Visser, 2016). Neutrophil depletion studies in both transplantable and spontaneous mouse tumor models have shown decreased growth in several tumor types (reviewed in (Coffelt et al., 2016; Galdiero et al., 2013)). One explanation for these conflicting results is that neutrophils alter their activity depending on their environment. Secretion

of TGFβ, G-CSF, and IFNβ by tumor and/or stromal cells can activate a pro-tumoral and metastastic agenda in neutrophils leading to immunosuppressive activity (Coffelt et al., 2016). Factors secreted by hypoxic cells can also induce neutrophil recruitment to metastatic sites even in absence of a primary tumor (Sceneay et al., 2012).

Metastasis is an area of carcinogenesis where neutrophils are suspected to play a role. Tumor-entrained neutrophils accumulate in metastatic sites prior to the arrival of metastatic cells, a phenomena referred to as "seeding," whose impact on tumorigenesis appears to be context-dependent (Granot et al., 2011; Liang & Ferrara, 2016). Further studies suggest that neutrophils participate in multiple steps of metastasis including intravasation, survival in circulation, and extravasation, acting as a guide for cancer cells (reviewed in (Coffelt et al., 2016; Liang & Ferrara, 2016).

CXCL1, a chemokine mediating neutrophil recruitment, can be secreted by multiple components of the tumor microenvironment including leukocytes and senescent cells (Coppe, Desprez, Krtolica, & Campisi, 2010; De Filippo et al., 2013). Senescent cells are cells exposed to high levels of stress who undergo irreversible growth arrest and develop a senescence-associated secretory phenotype (SASP). During the development of the SASP, a senescent cell can dramatically change its metabolic activity to begin secretion of soluble signaling factors such as interleukins, chemokines, and growth factors, as well as proteases and insoluble proteins (Coppe et al., 2010). The SASP is a dynamic process, which can differ in cell type, type of senescence, and even may change in the same cell over time (Coppe et al., 2010). While senescent growth arrest is driven by p53 and $p16^{INK4a}$, its SASP activity is activated primarily through the NF-κB pathway, which is negatively regulated by p53 (reviewed in (Salminen, Kauppinen, & Kaarniranta, 2012)). SASP factors have both autocrine and paracrine functions. In the secreting cell, SASP

serves to further promote senescence, and in neighboring cells SASP factors can induce senescence, drive infiltration of immune cells, and effect cell differentiation (Hoare & Narita, 2013). In healthy tissue, SASP promotes repair after injury, however persistent inflammation can lead to deleterious effects (Coppe et al., 2010; Saleh et al., 2018). SASP mediated immune-cell infiltration is likely due to the secretion of cytokines such as IL-6, IL-1, IL-8, TGF-β, CSF-1, CXCL-1, MCP-1, and ICAM-1 (Coppe et al., 2010; Hoare & Narita, 2013). While immune cells are necessary to clear senescent and dead cells, their persistence can become problematic, as seen in hepatocellular carcinoma, where senescent-recruited $CCR2^{+}$ myeloid cells accelerate tumor growth through NK cell inhibition (Eggert et al., 2016). Additionally, SASP has been shown to affect the stem cell niche and may permit emergence of cancer stem cells (Cahu, Bustany, & Sola, 2012; Milanovic et al., 2018; Mosteiro et al., 2016).

Most tumor microenvironment studies focus on tumors in peripheral tissues, which can differ significantly compared to the central nervous system (CNS). Several factors contribute to this, including the presence of tissue-resident cell types such as microglia, the blood-brain-barrier, which keeps the CNS relatively immune privileged, and a stiffer extracellular matrix, which can further prevent T cell infiltration (Quail & Joyce, 2017). Nevertheless, brain tumor microenvironment may contain endothelial cells, pericytes, fibroblasts, and immune cells, with macrophages representing the majority of the TME, and in some cases contributing to 30% of the tumor mass (Quail & Joyce, 2017). While it can be difficult to distinguish between microglia and bone-marrow derived macrophages (BMDM) that have infiltrated the tumor, like in breast and pancreatic cancers, it has been demonstrated in glioma mouse models that both populations contribute to the TAMs, and may play different roles in tumor growth (Bowman et al., 2016). Immunohistochemical analyses of human tissue has revealed that these TAMs produce low levels

of pro-inflammatory cytokines and lack expression markers for T cell co-stimulation, suggesting deficiency in tumor clearance (Hussain et al., 2006).

Medulloblastoma

From late embryogenesis to early postnatal development, cerebellar granule neurons proliferate rapidly to become the most numerous cells of the brain. This period of proliferation is induced by purkinje cell secretion of the mitogen Sonic Hedgehog (Shh), which binds to the receptor Ptch1 on the granule cell progenitors (GCPs). Upon binding of Shh, Ptch1 releases its inhibition on the receptor Smoothened (SMO), permitting activation of Gli, a family of transcription factors that induce cell proliferation (Wechsler-Reya & Scott, 1999).

In rare cases, disruption of this process leads to medulloblastoma. Medulloblastoma is a high-grade malignant tumor that forms from GCPs in the posterior fossa and represents the most common form of pediatric brain cancer (Louis et al., 2016). In recent years, medulloblastoma has been divided into four molecular subgroups: SHH, Wnt, Group 3, and Group 4, which differ in mechanisms and clinical aspects. The SHH subgroup, which makes up approximately 30% of medulloblastoma cases, is characterized by aberrant Shh signaling. Mutations in the Shh signaling pathway are associated with these tumors, most commonly in *Ptch1*, and less frequently in *SMO*, and *SUFU* (Taylor et al., 2012).

Standard of care treatment includes surgery, chemotherapy, and radiation, resulting in a 60-80% five-year overall survival rate for the SHH group (Northcott et al., 2012). Sadly these aggressive treatments confer a risk for developing secondary cancers, and leave many patients with lasting neurologic deficits that may hinder their ability to thrive in life. While SMO targeted therapies have shown promise in treating SHH medulloblastoma, case studies have demonstrated that the response is only transient due to acquired resistance (Metcalfe & de Sauvage, 2011; Yauch

et al., 2009). Thus, there is a push to better understand the molecular mechanism and environment of this tumor in order to facilitate the development of more effective treatments.

The tumor microenvironment of medulloblastoma has not been well-characterized. Our lab has shown that senescent cells are present in pre-malignant, preneoplastic lesions, and the evasion of senescence through mutations in p53 or alterations in $p16^{INK4a}$ lead to medulloblastoma progression (Tamayo-Orrego et al., 2016). Whether these cells are affecting the microenvironment has yet to be explored. Several studies in the late 20^{th} century described the presence of macrophages in human medulloblastoma biopsies (Morantz, Wood, Foster, Clark, & Gollahon, 1979; Roggendorf, Strupp, & Paulus, 1996; Rossi et al., 1991). Also using biopsy samples, a study in 2014 showed that macrophage infiltration was elevated in the SHH group compared to the other subgroups, and that areas of macrophage infiltration correlated with areas of proliferation (Margol et al., 2015). Using immunohistochemistry on SHH medulloblastoma biopsies, a study in 2018 suggested that M1 macrophage recruitment correlated with worse overall survival (Lee et al., 2018). Tumor cells isolated from a desmoplastic medulloblastoma expressed CSF-1, and co-culture of the tumor cells and microglia led to increased proliferation in both populations (Papavasiliou et al., 1997). While the subtype of that tumor is unknown, it is likely that it belonged to the SHH subgroup, like majority of desmoplastic medulloblastomas (Taylor et al., 2012).

There have been few animal studies looking at medulloblastoma tumor microenvironment. A study in 2013 described the presence of STAT3-expressing MDSCs in a Smo-mutant Shh medulloblastoma model; and their conditional deletion of STAT3 suggested that these cells were curtailing the pro-inflammatory environment (Abad et al., 2013). In 2016, a study compared a Shh mouse model (orthotopic transplantation of $Ptch1^{+/-}$ GCPs) to a Group 3 mouse model (orthotopic transplantation of neural stem cells with p53 and myc mutations.) Compared to Group 3, the Shh

model showed increased infiltration of macrophages, neutrophils, and MDSCs, as well as increased PD-1 expression. However, neither anti-PD-1 nor anti-CTLA-4 treatments affected overall survival in the Shh model (Pham et al., 2016). Thus, further study to determine the role the tumor microenvironment in medulloblastoma is warranted.

Rationale

Targeting the tumor microenvironment has become an exciting therapeutic avenue which has been successful in several cancers. Clinicaltrials.gov currently lists over 1,000 actively recruiting interventional immunotherapy clinical trials. However, little is known about the specific microenvironment of SHH medulloblastoma. Using a spontaneous model of Shh medulloblastoma, the $Ptch1^{+/-}$ mouse, we aimed to characterize and manipulate the tumor microenvironment to study its role in tumorigenesis. We focused on the following questions:

1. What immune cells are present in medulloblastoma preneoplasia and advanced tumors?
2. What effect does peripheral macrophage depletion have on preneoplasia and tumor growth?
3. Do senescent cells affect the tumor microenvironment and tumor growth?

Methodology

Mice

All animal work was performed according to the Canadian Council on Animal Care guidelines. $Ptch1^{+/lacZ}$ (referred to as $Ptch1^{+/-}$) mice were backcrossed with C57BL/6 mice. Preneoplasia samples was taken at postnatal day (P) 14-21, advanced tumors were taken upon demonstration of symptoms, around P200. For harvesting tissue, mice received 0.1mL/10g ketamine/xylazine prior to intracardiac perfusion with 0.9M NaCl. Tissue was fixed in 4% paraformaldehyde (PFA) in phosphate buffer at 4◦ for 18 hours, then incubated in 30% sucrose in phosphate buffer saline (PBS) for 24-48 hours. Tissue was frozen in a block of OCT and sectioned at 12μm thickness.

Drug Treatments

Clodronate and PBS liposomes were purchase from Liposoma B.V. For short-term peripheral macrophage ablation: mice received 3 injections of 10uL/g either clodronate or PBS liposomes. The injections were administered intraperitoneal every 3 days, starting on P12 and ending on P18. Mice were sacrificed on P19 for analysis. For long-term peripheral macrophage depletion: mice received 9 injections of 10uL/g either clodronate or PBS liposomes. The injections were administered intraperitoneal every 5 days, starting on P21 and ending on P62. Mice were sacrificed on P64/P65 for analysis.

ABT-263 (Navitoclax) was purchased from Selleck Chemistry (Catalog No. S1001) and dissolved in 5% DMSO and corn oil. Mice received either vehicle or ABT-263 at 55mg/kg via oral gavage for 5 consecutive days, starting on P14, and ending on P18. Mice were sacrificed on P19 for analysis.

Immunofluorescence/Immunohistochemistry

Slides were permeabilized with 0.3% Triton, incubated in 10% goat or donkey blocking buffer + 0.1% Triton for 1 hour, then incubated in primary antibody overnight. Secondary antibody was applied for 1 hour at room temperature. Antibodies: anti-Ki67 (ab16667, 1:1000), anti-p16 (ab54210, 1:200), anti-p21 (ab7960, 1:200), anti-Sox2 (ab97959 – 1:1000, ab79351 – 1:500) were purchased from Abcam; anti-CD80 (561955, 1:100), anti-CD86 (553692, 1:100), anti-NK-1.1 (553162, 1:1000) were purchased from BD Biosciences; anti-CD19 (115511, 1:100), anti-F4/80 (123102, 1:100), anti-Ly6G (127609, 1:100), anti-Mac2 (125410, 1:100) were purchased from Biolegend; anti-cleaved caspase-3 (9661s, 1:1000) was purchased from Cell Signaling; anti-CD11c (17-0114-82, 1:100), anti-MHCII (14-5321-82, 1:100) were purchased from eBioscience. Fluorescently conjugated secondary antibodies were purchased from Jackson ImmunoResearch and used at 1:1000 concentration.

Cell Culture

GCP isolation was performed as previously described (Mille et al., 2014). GCPs were cultured in Neurobasal supplemented with B27 (GIBCO), 0.5mM L-glutamine (GIBCO), and penicillin/streptomycin, and seeded onto plates pre-coated with 100µg/ml poly-D-lysine (Sigma).

Mouse embryonic fibroblasts (MEFs) were cultured in DMEM + Glutamax (GIBCO), 10% fetal bovine serum (Multicell), 1% penicillin/streptomycin (Invitrogen). To induce senescence in MEFs, near-confluent cells were exposed to either 10 Gy γ-irradiation or 2 hours of 150µM H_2O_2, then fixed 10 days later with 4% PFA for 15 minutes, changing the media every three days.

Publicly Available Data Usage

R2: Genomics Analysis and Visualization Platform (http://hgserver1.amc.nl/cgi-bin/r2/main.cgi) was used for analysis of gene expression, using data from *Cavalli, FMG et al., Cancer Cell 2017*. Two tailed t tests were calculated and displayed on the webpage. Dataset: Tumor Medullolbastoma – Cavalli – 763 0 rma_sketch – hugene11t was used.

Statistical Analysis

Data is expressed as mean ± SEM and was analyzed using R or GraphPad Prism 7. Graphs were generated in PRISM 7 (GraphPad). Statistical significance is: n.s. = not significant, *p≤0.05, **p≤0.01, ***p≤0.001, ****p≤0.0001.

Research Findings

To investigate the microenvironment, we performed immunostainings on preneoplastic and advanced tumor tissue, using wild-type spleen tissue from postnatal-day (P) 21 mice as a positive control. We used the following markers: F4/80 (pan-macrophages), Ly6G (neutrophils), and CD19 (B cells). We also tested markers for TCRβ (T cells), NK-1.1 (NK cells), and CD11c (dendritic cells), but the spleen immunostainings were inconclusive, so we cannot conclude the presence or absence of these cells in our lesions (data not shown). In advanced tumors, we found an abundance of macrophages and neutrophils (n>10, Figure 1A). In preneoplasia, we found macrophages but not neutrophils (n>10, Figure 1A). We suspect the absence of neutrophils is related to stage or timing rather than size, as even uncharacteristically large lesions obtained during the window of preneoplasia were also all devoid of neutrophils (n=5, Figure 1B). We did not see B cells in either preneoplasia or advanced tumors (n=3, Figure 1A).

Using publicly available data published in 2017 that contained 763 medulloblastoma samples, including 223 of the SHH subgroup, we compared immune cell gene transcripts of the SHH subgroup to the others (Cavalli et al., 2017). Compared to the other subgroups, SHH showed significantly higher expression of macrophage gene CD14, and helper T cell marker CD4, as well as slight but significantly higher expression of neutrophil-related gene CEACAM8 (Figure 1C). There was slight, but significantly lower expression of cytotoxic T cell gene CD8A, NK cell gene NCR1, and B cell gene CD19 (Figure 1C). There was no significant difference in dendritic cell gene ITGAX (Figure 1C). The immunostaining and gene expression results are summarized in a table in Figure 1D.

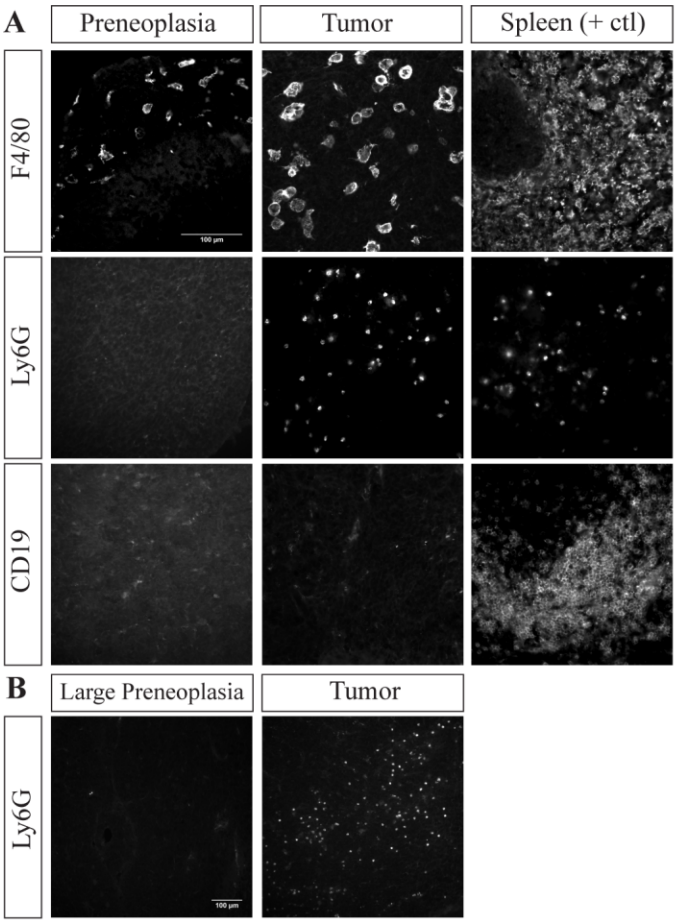

D

Cell Type	Macrophage	Neutrophil	T Cell	NK Cell	Dendritic Cell	B Cell
Antibody tested	F4/80 Iba1 CD45 CD11b	Ly6G Ly6C	TCRβ	NK-1.1	CD11c	CD19
Signal in Preneoplasia?	Yes	No	Inconclusive	Inconclusive	Inconclusive	No
Signal in Tumor?	Yes	Yes	Inconclusive	Inconclusive	Inconclusive	No
Signal in Spleen?	Yes	Yes	Inconclusive	Inconclusive	Inconclusive	Yes
Gene	CD14	CEACAM8	CD8A CD4	NCR1	ITGAX	CD19
Shh vs other groups?	Increase	Slight increase	CD8: Slight increase CD4: Increase	Slight decrease	No difference	Slight decrease

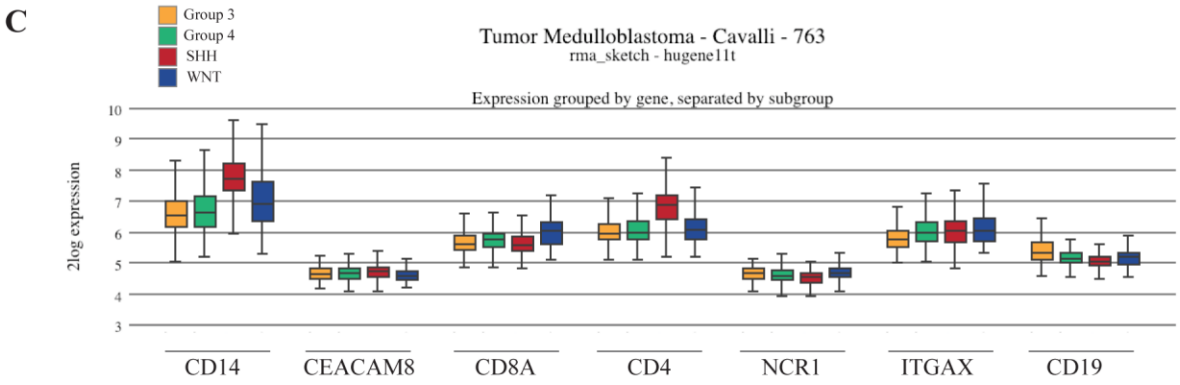

Figure 1. Shh medulloblastoma has a unique and evolving tumor microenvironment that includes macrophages and neutrophils

(A) Immunofluorescence (IF) images on preneoplastic and advanced tumor Ptch1$^{+/-}$ mouse sections, wild-type spleen used as a positive control (F4/80 n>10, Ly6G n>10, CD19 n=3).

(B) IF on large preneoplasia (n=5), and advanced tumors (n>10)

(C) Graph displaying gene expression from publicly available data from analyzed using R2 Genomics Analysis and Visualization Platform shows different immune cell gene expression across the four medulloblastoma subtypes.

(D) Summary table of immunostainings and gene expression analysis

To explore the role of the macrophages in the tumor, we stained Ptch1$^{+/-}$ tumor sections with markers associated with M1 or M2 polarization. For M1 polarization we used markers associated with pro-inflammatory T-cell costimulation: CD80, CD86, MHCII; for M2 polarization we used marker Mac2 associated with tissue repair. Tumors appeared negative for CD80 and CD86, however we cannot draw conclusions from these immunostainings due to lack of a positive control to verify the antibodies (data not shown). We observed both MHCII^{+} and Mac2^{+} cells, which always colocalized with the pan-macrophage marker F4/80, suggesting there are both M1-like and M2-like macrophages in the tumors (n=4, Figure 2A). MHCII and Mac2 seldom colocalized, suggesting heterogeneity in the TAM population (Figure 2A). MHCII and Mac2 immunostainings were also done separately without F4/80 to confirm the results were not due to fluorescent channel cross-talk (data not shown).

In every advanced tumor we analyzed (n>10), we saw large aggregates of macrophages (Figure 2B-D). To see if these were areas of proliferation, we costained with Ki67, a marker of proliferation, and F4/80. We did not see any Ki67^{+}F4/80^{+} colocalization, and strikingly, the areas of aggregated macrophages were completely devoid of Ki67^{+} tumor cells (Figure 2B). We suspected that these might represent areas of necrosis in the tumors. To see if the areas were populated by cell death, we costained tissue with apoptosis marker cleaved caspase-3 and F4/80. In contrast to our results with Ki67, the areas containing macrophage aggregates were strongly positive for caspase-3, suggesting that macrophages are clustering in regions of high cell death (Figure 2B). DAPI staining shows these areas clustered with pyknotic cells, further supporting that these are foci of cell death (Figure 2C). However, it is unclear if the macrophages are exerting pro- or anti-inflammatory activity in these regions. When we costained for M1 and M2 markers, we found that the macrophage aggregates contained mostly Mac2^{+}MHCII^{-}F4/80^{+}, with some

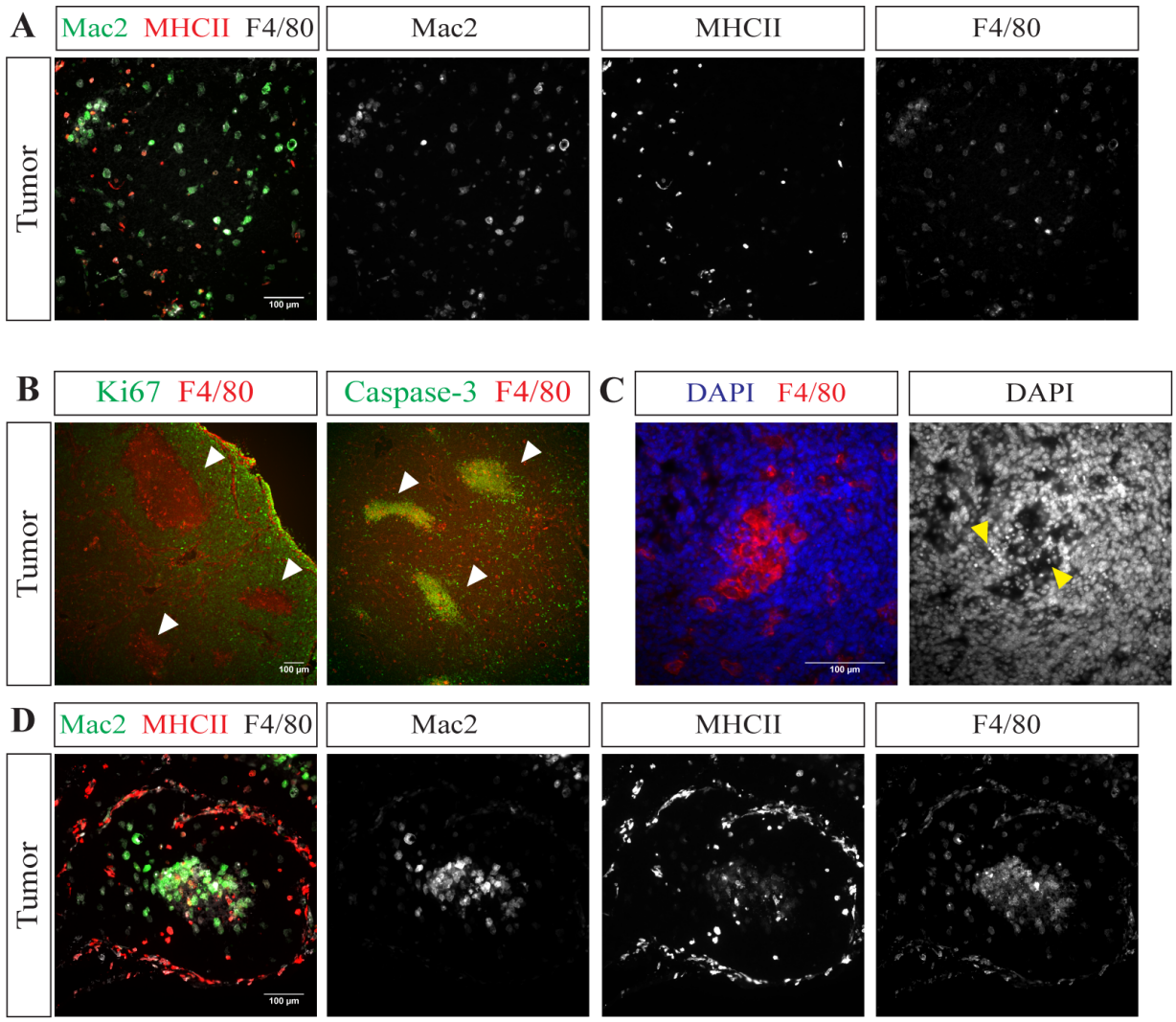

Figure 2. M1-like and M2-like macrophages aggregate in apoptotic regions of the tumor
(A) IF of Ptch1$^{+/-}$ advance tumors using macrophage markers Mac2, MHCII, and F4/80 (n=4).
(B) IF showing macrophage aggregates are Ki67^{-} (n=1).
(C) IF showing macrophage aggregates are caspase-3^{+} (n=1).
(D) IF showing macrophage aggregates contain pyknotic cells (n>10).
(E) IF showing macrophage aggregates contain Mac2^{+}MHCII^{-}F4/80^{+}, Mac2^{-}MHCII^{+}F4/80^{+}, and Mac2^{-}MHCII^{-} F4/80^{+} cells (n=4).

Mac2^{-}MHCII^{+}F4/80^{+} and Mac2^{-}MHCII^{-}F4/80^{+} cells (Figure 2D). This may suggest that the aggregates are not exerting a strong anti-inflammatory response, but further functional experiments are needed to test this.

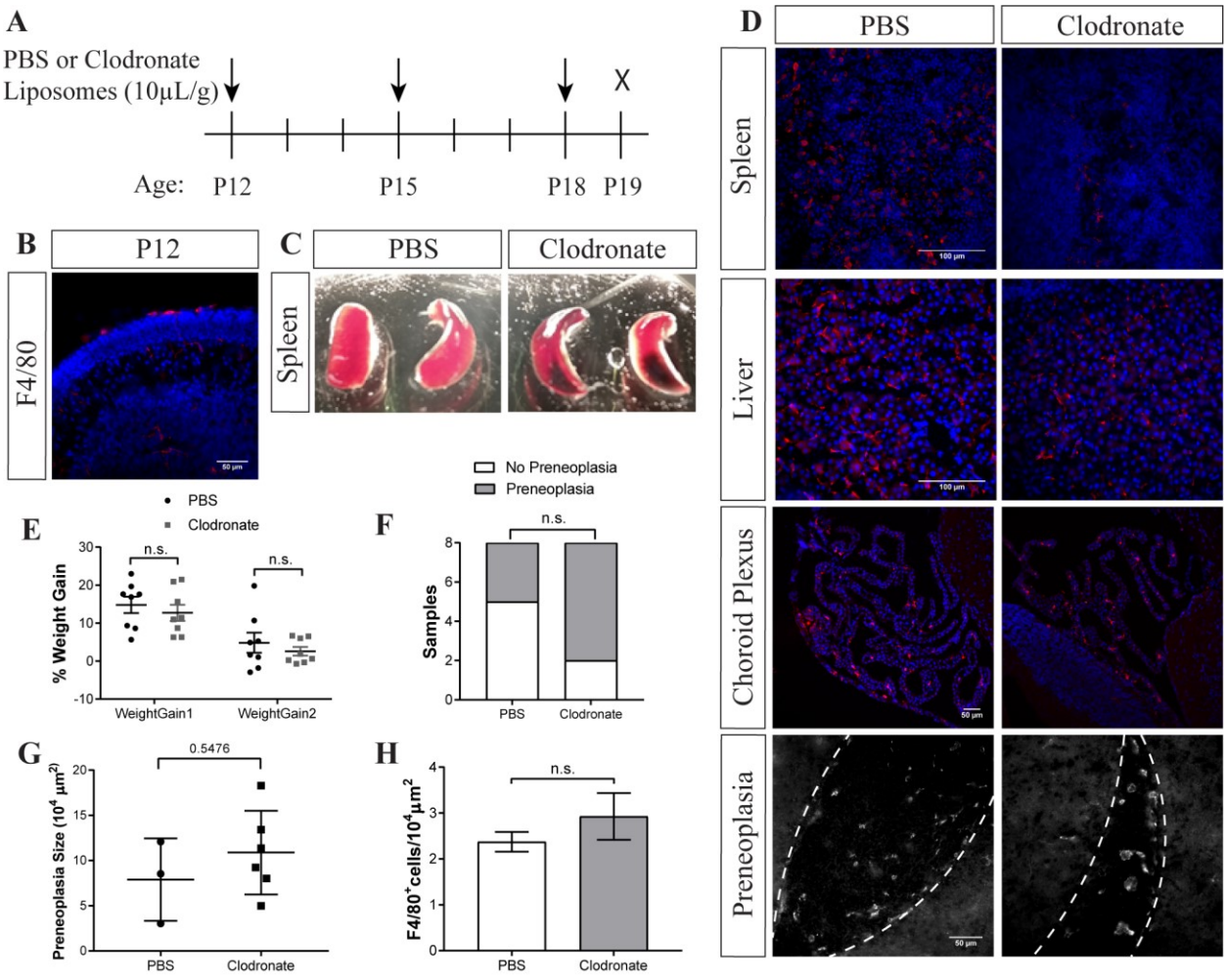

Figure 3. TAMs are the preneoplastic stage are primarily microglia

(A) Schematic depicting treatment schedule. Ptch1$^{+/-}$ mice were treated with 10uL/g PBS or Clodronate liposomes starting on P12, then repeated twice every 3 days. Mice were sacrificed for analysis on P19.

(B) Immunostaining shows F4/80^{+} are absent from the EGL at P12 (n=4). Dashed line shows outline of EGL.

(C) Image of spleens from PBS and clodronate treated mice. Clodronate treated spleens show discoloration at the proximal end (n=2).

(D) F4/80 immunostaining on P19 PBS or Clodronate treated mice, showing spleen and liver (positive control n=4), choroid plexus (negative control n=8), and preneoplasia (PBS: n=3, Clodronate: n=6). Dashed lines indicate outline of preneoplasia.

(E) Plot showing percent weight gain in PBS and Clodronate groups between injections 1-2 and 2-3 (PBS weight gain 1 = 14.8%±2.158, Clodronate weight gain 1 = 13.96%±1.911, PBS weight gain 2= 4.825%±2.631, Clodronate weight gain 2 = 3.59%±1.21. Unpaired t test p=0.7742, p=0.6538, respectively, n=8).

(F) Preneoplasia incidence between PBS and Clodronate groups (two-tailed Fischer's exact test p=0.3147, n=8).

(G) Plot comparing preneoplasia size between PBS and Clodronate treated mice, (two-tailed Mann Whitney test, p=0.5476, n=3, n=6, respectively).

(H) Bar graph comparing density of F4/80+ cells in preneoplasia (PBS = 2.373±0.215, Clodronate = 2.927±0.510, unpaired t-test p=0.4904, n=3, n=6 respectively).

It is unclear if the TAMs in the preneoplasia are solely microglia-derived or if peripheral macrophages have infiltrated into the tumor, as seen in glioma models (Bowman et al., 2016). To study the identity and function of macrophages on preneoplasia, we performed a macrophage depletion experiment. We administered 10μL/g clodronate liposomes or PBS liposomes to P12 $Ptch1^{+/-}$ mice every three days for a total of three injections (Figure 3A). Given that the clodronate liposomes cannot pass the blood-brain-barrier, and SHH has an intact blood brain barrier, we suspected this would deplete only peripheral macrophages, while leaving microglia unperturbed (Phoenix et al., 2016). Notably, macrophages were absent from the EGL at P12, but abundant by P21 (n=4, Figure 3B, Figure 1A). The clodronate treatment was well-tolerated by the mice, who showed no difference in overall health or weight gain when compared to the PBS group (n=8, Figure 3E). However, unlike PBS treated mice, the spleens of clodronate treated mice showed discoloration at the proximal end, possibly due to accumulation of uncleared red blood cells (Figure 3C). The clodronate treated mice had dramatic reduction of splenic and liver macrophages (n=4), but no change in choroid plexus and brainstem microglia (n=8) indicating that the drug successfully depleted peripheral macrophages while leaving CNS-macrophages untouched (Figure 3D). The clodronate treated mice had a higher incidence of preneoplasia when compared to PBS treated mice, but it was not significant (n=8, Figure 3F). There was no significant difference in preneoplasia size between the PBS and clodronate conditions (PBS n=3, clodronate n=6, Figure 3G). We also saw no significant difference in preneoplasia macrophage density between the clodronate and PBS treated conditions (PBS n=3, clodronate n=6, Figure 3D,H). Together this shows that peripheral macrophage depletion may affect medulloblastoma incidence, but does not affect preneoplasia size or macrophage density, and suggests that at the preneoplastic stage the $F4/80^{+}$ cells are of microglial origin, rather than peripherally-derived.

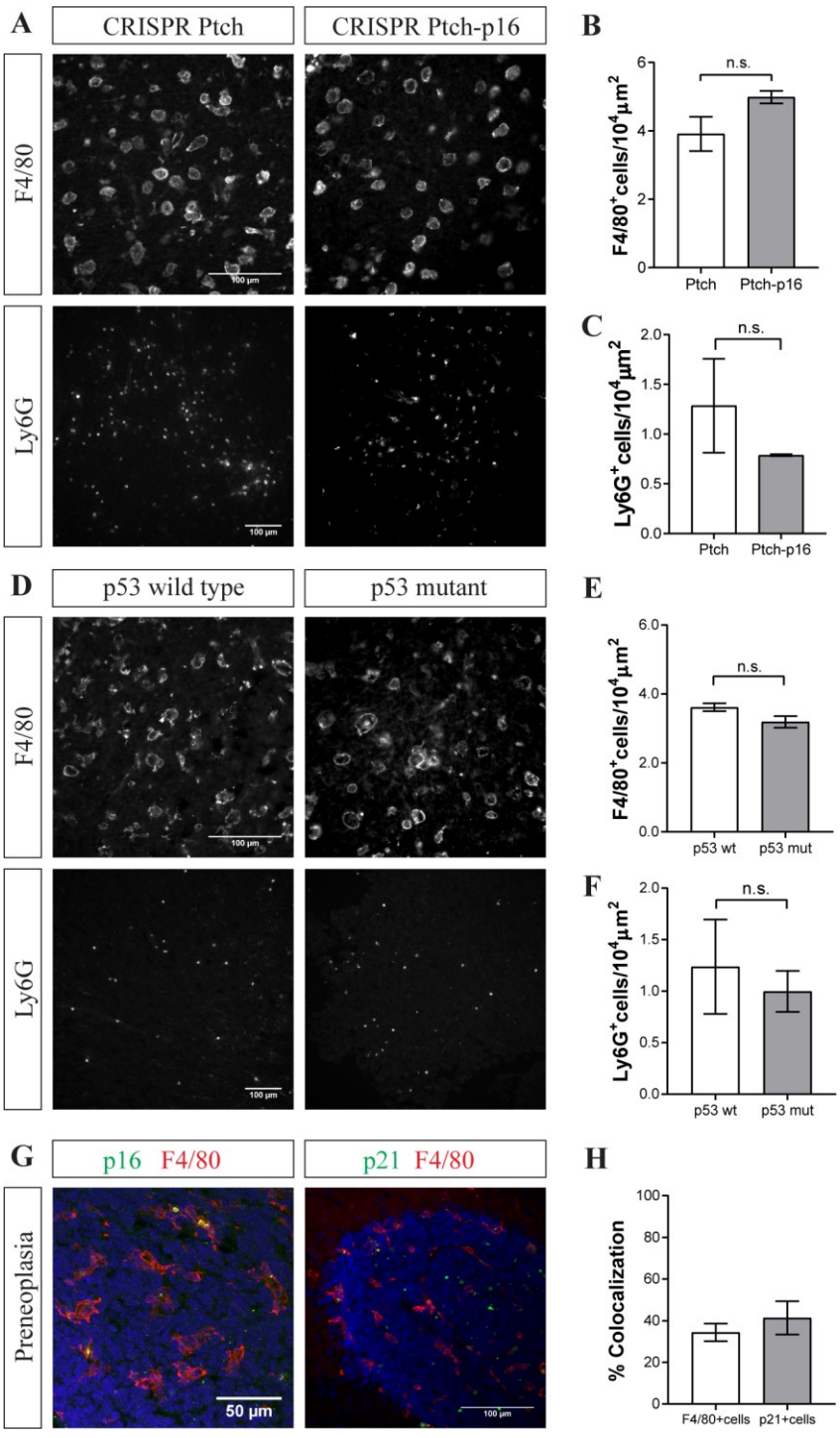

Figure 4. Senescent cells do not affect immune cell infiltration

(A) F4/80 and Ly6G immunostaining on in-utero electroporation (IUE) tumors generated by using CRISPR-Ptch1 or CRISPR-Ptch-p16 DNA

(B) Graph comparing F4/80^{+} cell density between CRISPR-Ptch1 and CRISPR-Ptch-p16 IUE generated tumors (CRISPR-Ptch=3.913±0.503, n=4; CRISPR-Ptch-p16=4.988±0.184, n=3; unpaired t test p=0.1154).

(C) Graph comparing Ly6G^{+} cell density between CRISPR-Ptch1 and CRISPR-Ptch-p16 IUE generated tumors (CRISPR-Ptch =1.285±0.472, n=4; CRISPR-Ptch-p16=0.788±0.008, n=3; unpaired t test p=0.5215).

(D) F4/80 and Ly6G immunostaining on p53 wild-type and p53 mutant tumors.

(E) Graph comparing F4/80^{+} cell density between p53 wild type and p53 mutant tumors (p53 wt = 3.614±0.113, n=3; p53 mut = 3.19±0.167, n=3; unpaired t test p=0.1155).

(F) Graph comparing Ly6G^{+} cell density between p53 wild type and p53 mutant tumors (p53 wt = 1.237±0.459, n=3; p53 mut = 0.998±0.199, n=3; unpaired t test p=0.658).

(G) IF using F4/80 and senescent markers, p16 and p21, on Ptch1$^{+/-}$ preneoplastic tissue sections.

(H) Graph displaying percent of total F4/80+ and p21+ cells that colocalized with each other (F4/80+ cells colocalized with p21 = 34.43±4.22%, p21+ cells that colocalize with F4/80 = 41.37±7.99%; n=5).

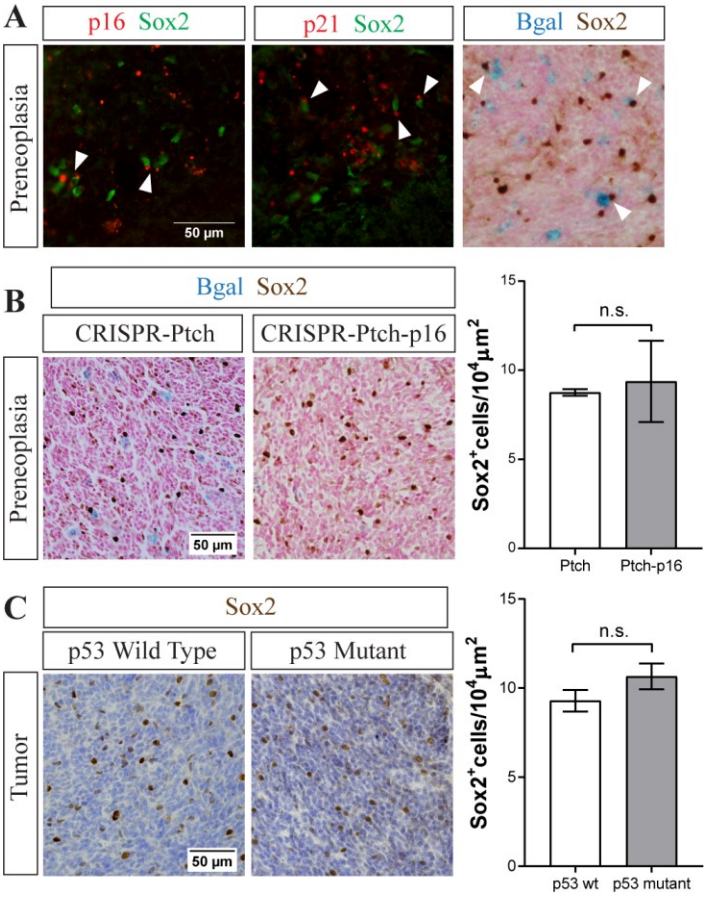

Figure 5. Senescent cells do not influence the stem cell niche

(A) Immunostaining and immunohistochemistry using Sox2 and senescent markers, p16, p21, beta-galactosidase (Bgal) on Ptch1$^{+/-}$ preneoplasia.

(B) Bgal staining and Sox2 immunohistochemistry on CRISPR-Ptch1 and CRISPR-Ptch1-p16 IUE tumors. Sox2 density quantification shows no significant difference, (CRISPR-Ptch=8.755± 0.182, n=4; CRISPR-Ptch-p16= 9.375±2.276, n=3; unpaired t test).

(C) Bgal staining and Sox2 immunohistochemistry on p53 wild type and p53 mutant Ptch1$^{+/-}$ tumors. Sox2 density quantification shows no significant difference, (p53 wt = 9.286±0.600, n=6; p53 mut = 10.654±0.728, n=3; unpaired t test, p=0.2091).

To investigate the role of senescent cells on the tumor microenvironment, we generated lesions with CRISPR-Ptch1, and CRISPR-Ptch+p16^{INK4a} DNA via in-utero electroporation (done by Chia-Lun Wu in the lab). The CRISPR-Ptch1 was the control, like our Ptch1$^{+/-}$ mouse model, which develops preneoplasia, then evades senescence to form advanced tumors. The CRISPR-Ptch1-p16^{INK4a} is a model that bypassed senescence and showed rapid tumor growth, effectively skipping the preneoplastic stage (analysis done by Lukas Tamayo-Orrego, data unpublished). We hypothesized that if senescent cells were affecting the microenvironment, tumors that were senescent naïve would have an altered environment compared to tumors that previously had a population of senescent cells. Macrophage and neutrophil densities were not significantly different between the two groups (CRISPR-Ptch: n=4, CRISPR-Ptch-p16: n=3, Figure 4A-C). We also

compared the macrophage and neutrophil infiltration between p53 wild-type and p53 mutant tumors (mutations analyzed by Lukas Tamayo-Orrego), and saw no significant differences (n=3, Figure 4D-F). It should be noted that a small portion of cells were positive for both macrophage and senescence markers, but it is unclear which of those are senescent macrophages versus macrophages that have engulfed a senescent cell (Figure 4G). Approximately 35% of $F4/80^+$ cells colocalized with p21, and 41% of $p21^+$ cells colocalized with F4/80 (Figure 4H).

To explore the relationship between senescent cells and stem cells we stained preneoplasia for markers of senescence ($p16^{INK4a}$ and p21) and stem cells (Sox2). We noticed that the senescent and $Sox2^+$ cells were often within close proximity of each other (n=3, Figure 5A). To further explore this, we compared the number of Sox2 cells in the senescent evasion condition, CRISPR-Ptch1, to the senescent bypass condition, CRISPR-Ptch1-$p16^{INK4a}$, but saw no significant difference (CRISPR-Ptch1: n=4, CRISPR-Ptch1-p16: n=3, Figure 5B). Similarly, we compared the number of Sox2 cells in p53 wild-type and mutant tumors but saw no significant difference (p53 wild type: n=6, p53 mutant: n=3, Figure 5C).

Additionally, we tried to induce senescence by exposing GCPs to 0.15μM, 1.5μM, or 15μM H_2O_2 for 30 minutes or 60 minutes yet saw no significant increase in B-galactosidase activity when compared to the untreated condition (Figure 6D, E). For each experiment we used MEFs as a positive control for the SA-Bgal staining by inducing senescence with either 10Gy γ-irradiation or 150μM H_2O_2 (Figure 6B, irradiated MEF data not shown). Our impression from these experiments is that GCPs more readily undergo apoptosis than senescence when exposed to stress *in vitro*.

To further study the role of senescent cells in preneoplasia, we administered the Bcl-2/Bcl-XL inhibitor, ABT-263 (Navitoclax), to young mice to ablate senescent cells. ABT-263 was given at 55mg/kg/d for 5 days via oral gavage, starting on P14 and ending on P18. Mice were sacrificed

on P19 and analyzed (Figure 7A). The ABT263 treated mice tolerated the drug well, showing no difference in overall health or weight gain compared to the vehicle treated group (Vehicle: n=12, ABT263: n=8, Figure 7B). The incidence of preneoplasia was higher in the ABT263 treated mice (n=4/8) when compared to the vehicle treated mice (n=4/12), but it was not significant with Fischer's exact test (Figure 7C). Since macrophages can also express markers of senescence (Figure 4G), we quantified the $p21^{+}F4/80^{-}$ cells per 10^4 μm^2 to measure senescent cell ablation. While there was a trend for less $p21^{+}F4/80^{-}$ cells in the ABT263 treated cohort, this was not significant (Vehicle: n=3, ABT263: n=4, Figure 7D-E). It is possible this is due to the high variability in senescent cell density. Surprisingly, the ABT263 treated group had significantly larger preneoplasia size compared to the vehicle group (Vehicle n=4, ABT263: n=4, Figure F).

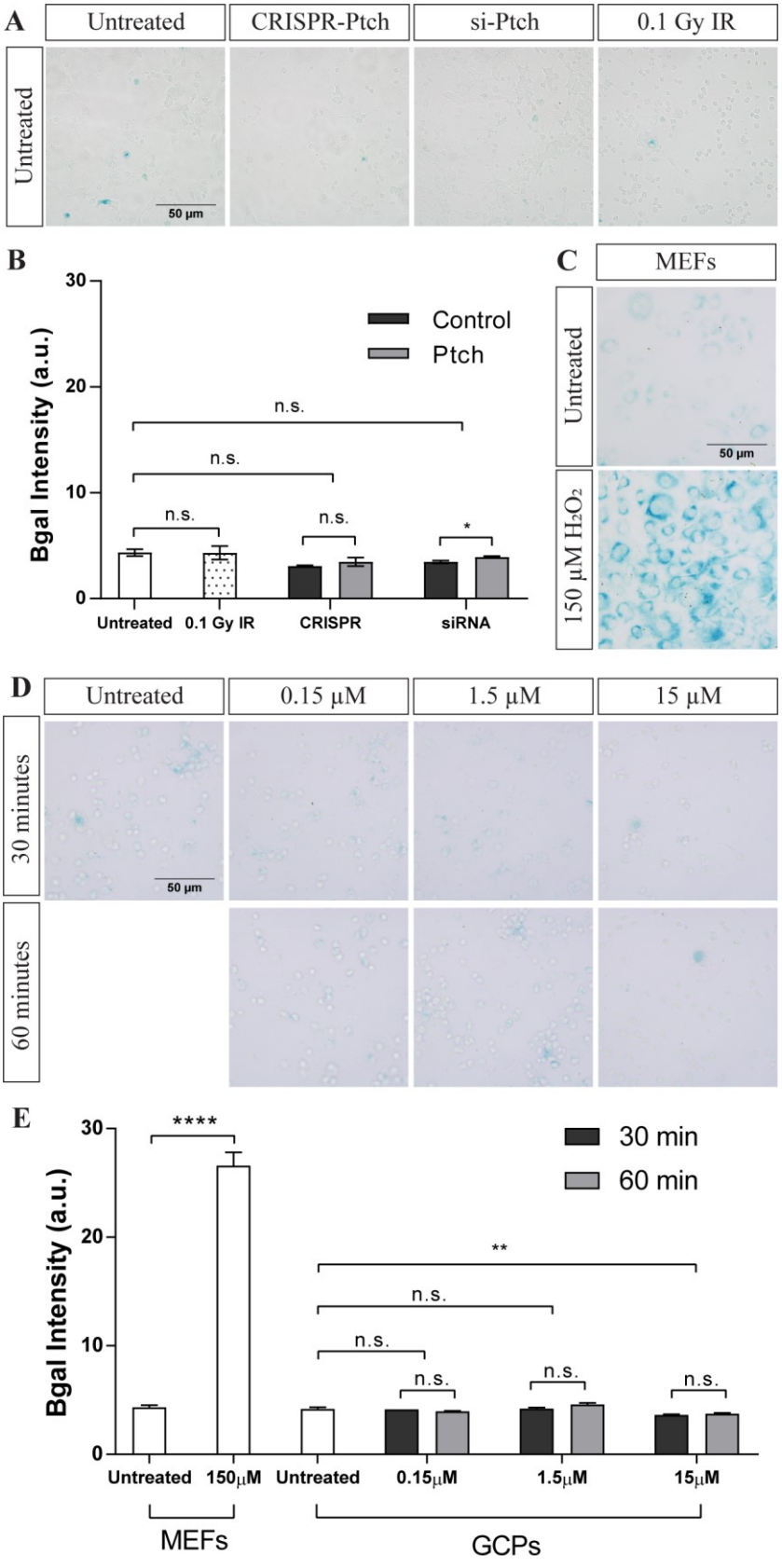

Figure 6. Granule cell precursors do not readily undergo senescence *in vitro*

(A) Bgal staining on GCPs. On the day of dissociation GCPs were either left untreated, transfected with CRISPR-Ptch DNA, transfected with siRNA targeting Ptch1, or exposed to 0.1Gy γ-irradiation. GCPs were then fixed on day 6 and stained for Bgal.

(B) Graph showing Bgal intensity for (A), (Untreated=4.35±0.324; 0.1 Gy IR = 4.33±0.634; Control CRISPR=3.072±0.069; CRISPR-Ptch=3.485±0.386; Control siRNA=3.468±0.140; Ptch siRNA = 3.950±0.087; unpaired t test, n.s.=p>0.05, *= p≤0.05).

(C) Bgal staining of untreated and H_2O_2 exposed MEFs (150uM H_2O_2, 2 hours)

(D) GCPs treated with either 30 minutes or 60 minutes of 0.15uM, 1.5uM, or 15uM H_2O_2 then fixed on day 5 and stained for Bgal

(E) Graph showing Bgal intensity for (C) and (D). (MEFS: Untreated=4.34±0.205; 150µM H_2O_2 = 26.595±1.22) (GCPs: Untreated=4.196±0.137; 0.15µM [30"] = 4.125±0.001; 1.5µM[30"] = 4.211±0.097; 15µM = 3.64±0.043; 0.15µM[60"] = 3.960±0.044; 1.5µM[60"] = 4.576±0.171; 15µM[60"] = 3.732±0.093; unpaired t test, n.s. = p>0.05, *=p≤0.05, ****=p≤0.0001).

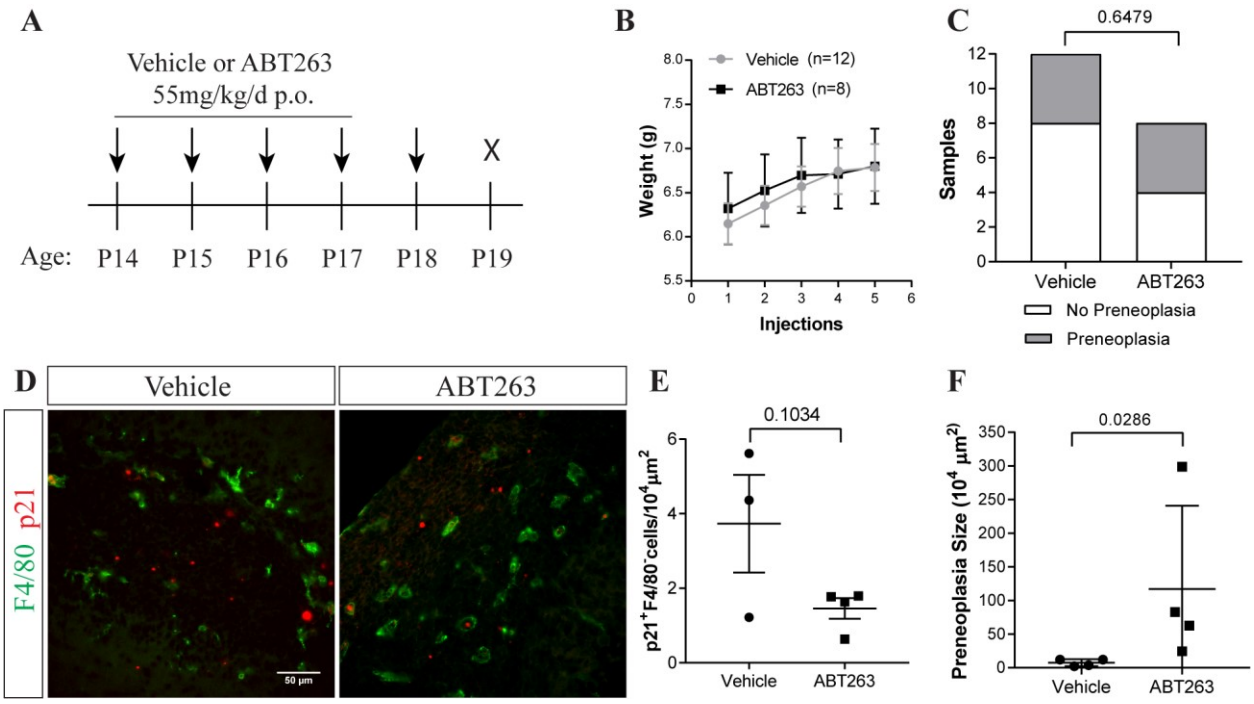

Figure 7. Ablation of senescent cells with Navitoclax increases preneoplasia size

(A) Schematic depicting treatment schedule. Ptch1$^{+/-}$ mice were treated with 55mg/kg/d ABT263 or Vehicle, administered oral gavage, for 5 days, starting on P14. Mice were sacrificed for analysis on P19.

(B) Plot showing weight over course of treatment for Vehicle and ABT263 treated mice.

(C) Preneoplasia incidence is not significant between groups (Vehicle: n=12, ABT263: n=8, two-tailed Fischer's exact test p=0.5238).

(D) F4/80 and p21 immunostaining on Vehicle and ABT263 treated tissue.

(E) Plot comparing p21^{+}F4/80^{-} cell density between Vehicle and ABT263 treated mice, (Vehicle=3.734±1.308, n=3; ABT263=1.462±0.277, n=4; two-tailed unpaired t test, p=0.103).

(F) Plot comparing preneoplasia size between Vehicle and ABT263 treated mice, (Vehicle=7.761±2.600, n=4; ABT263=72.77±61.76, n=4; two-tailed Mann Whitney test, p=0.5476).

Discussion of Findings

Using a Ptch1$^{+/-}$ mouse model, we have shown that the Shh subgroup has a unique and evolving tumor microenvironment. Cells expressing pan-macrophage markers populate the lesion from early to late development, and Ly6G-expressing cells infiltrate the tumors at advanced stages. Our evidence suggests that majority of the immune cells in the advanced tumors are macrophages, which is consistent with the reports of adult brain tumor immune cell infiltration (Bowman et al., 2016; Gentles et al., 2015; Pham et al., 2016; Quail & Joyce, 2017). Our immunostainings for T cells, NK cells, and dendritic cells were inconclusive (data not shown), so it would be interesting to perform FACS analysis using reliable markers for these cells to further characterize the immune cell types that may invade the tumors. It would be of great interest to stain for CD4^{+} T cells, given that the human expression data suggests the SHH subgroup has significantly higher infiltration compared to the other medulloblastoma subgroups. CD4^{+} T cells play a vital role in priming CD8^{+} T cells to fight tumorigenesis; but when deficient they dampen the cytotoxic response, offering a therapeutic target (Borst, Ahrends, Bąbała, Melief, & Kastenmüller, 2018). Thus, further experiments to investigate the activity of CD4+ T cells in SHH medulloblastoma would be valuable.

It is unclear if the Ly6G^{+} cells we observed in tumors are neutrophils or the alleged tumor-promoting MDSCs. The most convincing way to identify MDSCs is through observing their activity, rather than the markers they express, so it would be interesting to perform a co-culture with tumor cells to see if there is an effect on proliferation, survival, or motility. An interesting *in vivo* experiment to test if these cells are affecting tumor growth would be to deplete them with an anti-Gr-1 antibody. Comparing neutrophil infiltration between different subgroups of medulloblastoma such as WNT, which rarely metastasizes, to Group 3 and Group 4, which

frequently metastasis, would also be an interesting avenue to explore. Given the ambiguity of neutrophil/MDSC involvement in carcinogenesis, further study is warranted to uncover their role in medulloblastoma.

Depletion of peripheral macrophages at the preneoplastic stage did not affect TAM density, suggesting that the F4/80^{+} cells in preneoplasia are microglia. Uncovering TAM ontology is important because it may influence their activity and how they respond to the tumor microenvironment, as has been described in glioma and pancreatic adenocarcinoma (Bowman et al., 2016; Y. Zhu et al., 2017). One way to confirm our finding would be to use a microglia-specific marker to stain preneoplasia or FACS sort the F4/80^{+} cells. However there is no universally-accepted marker to reliably distinguish microglia from peripheral macrophages, partially due to the phenomena that peripheral macrophages may upregulate expression of microglia-specific markers upon infiltration (Bowman et al., 2016; Sevenich, 2018). Tmem119 and P2RY12 are two possible candidates, though their expression at P14 is ambiguous and their reliability to differentiate microglia from peripherally-derived TAMs is not well-described (Bennett et al., 2016; Bowman et al., 2016). A glioma model identified CD49 as a potential marker to discriminate microglia, which are CD49^{low}, from peripheral macrophages, which are CD49^{high} (Bowman et al., 2016). In our model, this experiment would need to be performed with FACS and paired with appropriate controls, such as circulating macrophages and microglia, to determine high versus low expression. Yet even with controls it may be difficult to draw strong conclusions if the result yields a homogeneous population. Mice expressing GFP in bone marrow could be used to test this as well, either through bone-marrow transplant to irradiated Ptch1$^{+/-}$ mice, or parabiosis with Ptch1$^{+/-}$ mice; techniques that have been used to study macrophage infiltration into the tissues (Franklin et al., 2014; Priller et al., 2001). These techniques introduce their own set of caveats though,

including disruption of the blood-brain-barrier and inflammation in irradiation models, and incomplete chimerism and ethical concerns for parabiosis models (Kierdorf, Katzmarski, Haas, & Prinz, 2013).

Whether microglia are affecting tumor growth is unclear. We showed that microglia are absent from the EGL of P7 mice but invade preneoplasia and have ameboid morphology between P14-P21. While embryonic and early postnatal microglia typically display ameboid morphology, by P14 their morphology should be highly ramified, suggesting the cells in the preneoplasia have active inflammatory activity (Giulian, 1987; Kaur, Rathnasamy, & Ling, 2017). To further explore this, one could directly administer clodronate liposomes to the brain via a cannula and measure the incidence and growth of preneoplasia and tumors. Another strategy would be to cross $Ptch1^{+/-}$ mice with the transgenic CX3CR1(CreER) mice, which allow for depletion of microglia upon administration of tamoxifen (Parkhurst et al., 2013). The presence of microglia has been described several times in brain tumors, though their functional role remains unclear and may be tumor specific (Sevenich, 2018).

While our evidence suggests that preneoplasia TAMs are microglia, the ontology of the TAM population in advanced tumors is unknown. As mentioned, macrophage ontology can influence TAM activity, and it is common for tumor microenvironments to evolve over time, thus further characterization of the TAM population is warranted. To investigate TAM ontology in tumors, we are currently undergoing a longer-course clodronate experiment where we deplete peripheral macrophages for six weeks and analyze if there is an effect on incidence or tumor size.

Most of the macrophages in advanced tumors express either Mac2 or MHCII, with minimal overlap. This suggests there is heterogeneity in the TAM population. Additional characterization of the macrophage population using other markers like the pro-inflammatory CD80 and CD86, or

pro-repair Arg1 would be interesting. It is possible that while some TAMs are acting to prevent tumor growth, others are promoting it, though that would need to be confirmed with functional experiments. It would be interesting to co-culture $Mac2^+$ and $MHCII^+$ TAMs with tumor cells to compare if there are effects on proliferation, differentiation, or if there is sustained cell-to-cell contact, as described in melanoma, which led to increased motility and metastasis (Roh-Johnson et al., 2017). If those results were promising, one could then test their effect *in vivo* through anti-Mac2 or anti-MHCII antibody-mediated depletion. Single-cell sequencing would also be a useful experiment here as it would further profile the heterogeneity and reveal if there are emerging groups of macrophages that can be identified by specific markers.

In advanced tumors, both $Mac2^+$ and $MHCII^+$ TAMs aggregate in regions of high cell death and low proliferation. Surprisingly, one study published that medulloblastoma TAMs are correlated with areas of high proliferation, which is contrary to our result (Margol et al., 2015). However, that study did not mention macrophage aggregates, which to our knowledge has yet to be described in medulloblastoma. Staining tumors with hypoxia markers such as pimonidazole or HIF-α would be interesting, as hypoxia can induce pro-tumorigenic activity in TAMs (Chen et al., 2009; Leblond et al., 2016; Mehrabi et al., 2018; Y. Zhu et al., 2017). Additionally, our evidence shows that most of the macrophages in the aggregates are $MHCII^-$, which are reportedly more susceptible to this hypoxia-mediated switch (Y. Zhu et al., 2017).

TAMs may affect checkpoint inhibitor activity, but the evidence suggests this is a complex process. For instance, one study showed that TAMs express PD-L1, which restrict CD8+ T cell activities, and depletion of TAMs enhanced T-cell mediated mammary tumor clearance when combined with chemotherapy (DeNardo et al., 2011). Supporting that, other studies in pancreatic, colorectal, and mammary tumor models demonstrated that combining macrophage depletion with

anti-PD1/anti-CTLA4 treatment showed a synergistic effect leading to tumor regression (Cassetta & Kitamura, 2018). However, a study in humans with melanoma showed that classic monocytes are actually required for effective responses to anti-PD1 therapies (Krieg et al., 2018). This further supports the idea that the population of TAMs can be heterogenous and play conflicting roles. Though Shh medulloblastoma did not respond to immune checkpoint inhibitors, perhaps that could be changed if given in combination with a drug to reprogram TAMs (Pham et al., 2016).

There are several strategies to target tumor-associated macrophages, including depletion, reducing recruitment, and reprogramming. Macrophage depletion, such as with clodronate or antibodies, is not clinically feasible due to the high toxicities that accompany immunosuppression (Cannarile et al., 2017). Reprogramming macrophages seems like the most desirable strategy, if one understands what type of macrophages to expect in a certain tumor microenvironment. This has been tested in several models and has shown some success. In a glioma mouse model, inhibition of CSF-1R affected macrophage polarization without decreasing the amount of macrophages, and saw reduced tumor growth (Pyonteck et al., 2013).

While writing this thesis a paper was published in Nature Communications on the tumor microenvironment of medulloblastoma (Maximov et al., 2019). Like the work presented in this thesis, they used the *Cavalli FMG et al., Cancer Cell 2017* dataset to show that the SHH subgroup had increased expression of macrophage markers compared to the other subgroups. They suggest that low expression of *AIF1* significant correlates with worse overall survival. It would be interesting to verify these findings in a validation cohort, as their expression cutoff was likely chosen based on what yielded the most significant p-value. Using a NeuroD2:SmoA1 as a mouse model, they confirmed our findings that the tumor microenvironment is composed of mainly myeloid cells, and to a smaller extent, neutrophils. Using the marker CD45 in FACS of tumors

they show that microglia and bone marrow derived macrophages (BMDM) make up the myeloid population in roughly equal proportions. With a transgenic mouse lacking *CCR2*, the gene encoding the receptor for the cytokine CCL2, they show that reduced macrophage infiltration correlates with worse overall survival, increased tumor cell proliferation, and decreased apoptosis. They also show that inhibition of CSF1 with two different inhibitors leads to decreased overall survival. Similar to our work, they used clodronate liposomes to manipulate macrophage infiltration. They administered clodronate to mice with orthotopic transplantation of tumor cells and saw decreased infiltration and increased proliferation. Surprisingly they did not mention in the manuscript if overall survival, tumor size, immune cell composition, or apoptosis was changed in the clodronate-treated mice, and this would be interesting to follow up on with our long-term clodronate experiment. Overall, they posit the model that early in tumorigenesis, microglia activated by tumor cells secrete CCL2, triggering infiltration of BMDM which have cytotoxic activity.

Our finding that microglia are the predominant myeloid cell at preneoplasia supports their model. While they do not describe the presence of macrophage aggregates in tumors, our results that macrophages correlate with regions of high apoptosis and low proliferation also support their findings. Unlike our work, they did not explore macrophage heterogeneity or tumor microenvironment evolution, which our results suggest is an interesting avenue. Additionally, their work focused on macrophages, leaving the role of neutrophils, senescent cells, and other components of the tumor microenvironment uncharted.

The fate of the senescent cells in preneoplasia and their effect on the tumor microenvironment is unknown. To study how senescent cells may affect the tumor-associated immune cells we used two models with manipulated senescence: the CRISPR-Ptch1-p16 allowed

us to look at tumors that bypassed senescence, therefore did not have senescent cells, and p53 mutated tumors, which may have unrestrained SASP due to the release of inhibition on NF-κB. Neither of these conditions showed a change in number of macrophages or neutrophils when compared to the appropriate controls, suggesting that immune cell infiltration is not strongly affected by the senescent cells in the lesions.

Initially we suspected that senescent cells may affect the stem cell niche, due to seemingly preferential location near each other during preneoplasia. However, we did not see an effect in the number of $Sox2^{+}$ cells when we looked at tumors that had bypassed senescence or had mutations in p53. We intended to further study the role of senescent GCPs *in vitro* but were unable to successfully induce senescence in GCPs despite efficient senescent induction in our positive controls, suggesting that GCPs do not readily undergo senescence in vitro. Given that the GCPs cannot reliably survive in culture for longer than 5-6 days, it is likely that we cannot culture them long enough to observe full senescence induction. We attempted to isolate senescent cells in culture from dissociating cerebella during the preneoplasia window, then FACS sorting $Ptch1^{+/-}$ p16-3MR mice for RFP+ cells but were unsuccessful (data not shown). We also tested an anti-DPP4 antibody, which would have been on the cell surface allowing for sorting, but were also unsuccessful (data not shown). Achieving senescence in GCPs in culture would be useful, as it could allow for experiments like a cytokine assay or qPCR to measure what factors are being secreted in the SASP. From that data, one would have a clearer direction to explore how the cells may be affecting the tumor microenvironment.

To further investigate the global role of senescent cells on the tumor microenvironment, we administered the senolytic drug Navitoclax to $Ptch1^{+/-}$ mice. As macrophages can express markers of senescence, we quantified the density of $p21^{+}F4/80^{-}$ cells and saw a trend for a decrease

in the Navitoclax treated mice. It's possible that this trend did not reach significance due to the small sample size and heterogeneity between the amount of senescence between lesions. We are continuing to increase our sample size for this experiment. Another possibility is that p21 is not the ideal marker to use for senescent cells in tissue. Unfortunately we could not use B-galactosidase as a marker since our Ptch1 mice express LacZ, and we tested seven p16 antibodies without success (data not shown).

Treatment with Navitoclax did not affect preneoplasia incidence but did increase the lesion size. One possibility is senescent cells induce senescence in their neighboring tumor cells. This would suggest that the SASP is primarily inhibiting tumor growth. If one could succeed to culture senescent GCPs, an interesting experiment would be to apply conditioned media from the senescent cells onto naïve GCPs and use qPCR to measure indicators of senescence such increased expression of $p16^{INK4a}$ or p21, or decreased expression of lamin B1. An *in vivo* experiment to explore this further would be to administer Navitoclax during the full window of preneoplasia (P14-P21) and observe if there is an effect on tumor size or survival.

Navitoclax functions as a senolytic because senescent cells upregulate inhibitory factors of intrinsic apoptosis, Bcl-XL and Bcl-2. However, cancer cells may also upregulate these factors in response to anti-cancer therapies, and Navitoclax is currently being investigated as a potential combination therapy for solid tumors (Gandhi et al., 2011). Considering that we did not treat the $Ptch1^{+/-}$ mice with any chemotherapeutic, the effect we observed is most likely due to the depletion of senescent cells. There are other senolytics that one could test to confirm this, such as dasatinib + quercertin (D+Q), flavone, fisetin, or other Bcl-XL inhibitors, though the type of senescent cells they target may differ and how senescent GCPs would respond is unknown (Yi Zhu et al., 2017; Zhu et al., 2015). Additionally, there are two transgenic mouse models that can be used to ablate

senescent cells: the p16-3MR mouse and the INK-ATTAC mouse (Baker et al., 2011; Demaria et al., 2014). Our lab is currently exploring these options to follow-up on this work.

Conclusion and Summary

The work presented in this thesis is an exploratory analysis of the tumor microenvironment of medulloblastoma, an area of study largely unexplored until recently. Overall, our work has further characterized the role of the tumor microenvironment of Shh medulloblastoma using the $Ptch1^{+/-}$ mouse model. We have shown that the microenvironment of preneoplasia contains microglia and senescent cells, and that senescent cells restrict preneoplasia growth. The tumor microenvironment changes as the tumor progresses to advanced stages, which show infiltration of neutrophils as well. Our lab is currently investigating how long-term peripheral macrophage and senescent cell depletion affects tumor growth.

That *Maximov V et al., Nature Communications, 2019* compliment and support our findings, even in a different mouse model of Shh medulloblastoma, is promising. Together these results open additional lines of study to further delve into the finer details of the tumor microenvironment, such as the potential of senescence-inducing drugs for restricting tumor growth, studying microglial and neutrophil involvement in tumor growth, and whether circulating neutrophil or monocyte numbers may serve as a non-invasive biomarker for patients in the clinic.

It is of the author's opinion that our model, the $Ptch1^{+/-}$ mouse, is an excellent tool to study the brain tumor microenvironment. Unlike many other models, the $Ptch1^{+/-}$ mouse develops tumors spontaneously, not requiring transplantation, irradiation, or immune incompetence, which can dramatically affect the immune cell interaction in the tumor (Qian & Pollard, 2010). Additionally, this model allows the study of initiation and progression, meaning one can study how the tumor microenvironment evolves as malignancy develops.

References

Abad, C., Nobuta, H., Li, J., Kasai, A., Yong, W. H., & Waschek, J. A. (2013). Targeted STAT3 disruption in myeloid cells alters immunosuppressor cell abundance in a murine model of spontaneous medulloblastoma. *Journal of leukocyte biology, 95*(2), 357-367. doi:10.1189/jlb.1012531

Baker, D. J., Wijshake, T., Tchkonia, T., LeBrasseur, N. K., Childs, B. G., van de Sluis, B., . . . van Deursen, J. M. (2011). Clearance of p16Ink4a-positive senescent cells delays ageing-associated disorders. *Nature, 479*(7372), 232-236. doi:10.1038/nature10600

Bennett, M. L., Bennett, F. C., Liddelow, S. A., Ajami, B., Zamanian, J. L., Fernhoff, N. B., . . . Barres, B. A. (2016). New tools for studying microglia in the mouse and human CNS. *Proceedings of the National Academy of Sciences, 113*(12), E1738. doi:10.1073/pnas.1525528113

Blaisdell, A., Crequer, A., Columbus, D., Daikoku, T., Mittal, K., Dey, S. K., & Erlebacher, A. (2015). Neutrophils Oppose Uterine Epithelial Carcinogenesis via Debridement of Hypoxic Tumor Cells. *Cancer Cell, 28*(6), 785-799. doi:10.1016/j.ccell.2015.11.005

Borst, J., Ahrends, T., Bąbała, N., Melief, C. J. M., & Kastenmüller, W. (2018). CD4+ T cell help in cancer immunology and immunotherapy. *Nature Reviews Immunology, 18*(10), 635-647. doi:10.1038/s41577-018-0044-0

Bowman, R. L., Klemm, F., Akkari, L., Pyonteck, S. M., Sevenich, L., Quail, D. F., . . . Joyce, J. A. (2016). Macrophage Ontogeny Underlies Differences in Tumor-Specific Education in Brain Malignancies. *Cell Rep, 17*(9), 2445-2459. doi:10.1016/j.celrep.2016.10.052

Cahu, J., Bustany, S., & Sola, B. (2012). Senescence-associated secretory phenotype favors the emergence of cancer stem-like cells. *Cell Death Dis, 3*, e446. doi:10.1038/cddis.2012.183

Cannarile, M. A., Weisser, M., Jacob, W., Jegg, A.-M., Ries, C. H., & Rüttinger, D. (2017). Colony-stimulating factor 1 receptor (CSF1R) inhibitors in cancer therapy. *Journal for ImmunoTherapy of Cancer, 5*(1), 53. doi:10.1186/s40425-017-0257-y

Cassetta, L., & Kitamura, T. (2018). Targeting Tumor-Associated Macrophages as a Potential Strategy to Enhance the Response to Immune Checkpoint Inhibitors. *Frontiers in Cell and Developmental Biology, 6*. doi:10.3389/fcell.2018.00038

Cavalli, F. M. G., Remke, M., Rampasek, L., Peacock, J., Shih, D. J. H., Luu, B., . . . Taylor, M. D. (2017). Intertumoral Heterogeneity within Medulloblastoma Subgroups. *Cancer Cell, 31*(6), 737-754 e736. doi:10.1016/j.ccell.2017.05.005

Chen, F. H., Chiang, C. S., Wang, C. C., Tsai, C. S., Jung, S. M., Lee, C. C., . . . Hong, J. H. (2009). Radiotherapy decreases vascular density and causes hypoxia with macrophage aggregation in TRAMP-C1 prostate tumors. *Clin Cancer Res, 15*(5), 1721-1729. doi:10.1158/1078-0432.CCR-08-1471

Coffelt, S. B., Wellenstein, M. D., & de Visser, K. E. (2016). Neutrophils in cancer: neutral no more. *Nat Rev Cancer, 16*(7), 431-446. doi:10.1038/nrc.2016.52

Coppe, J. P., Desprez, P. Y., Krtolica, A., & Campisi, J. (2010). The senescence-associated secretory phenotype: the dark side of tumor suppression. *Annu Rev Pathol, 5*, 99-118. doi:10.1146/annurev-pathol-121808-102144

De Filippo, K., Dudeck, A., Hasenberg, M., Nye, E., van Rooijen, N., Hartmann, K., . . . Hogg, N. (2013). Mast cell and macrophage chemokines CXCL1/CXCL2 control the early stage of neutrophil recruitment during tissue inflammation. *Blood, 121*(24), 4930. doi:10.1182/blood-2013-02-486217

Demaria, M., Ohtani, N., Youssef, S. A., Rodier, F., Toussaint, W., Mitchell, J. R., . . . Campisi, J. (2014). An essential role for senescent cells in optimal wound healing through secretion of PDGF-AA. *Dev Cell, 31*(6), 722-733. doi:10.1016/j.devcel.2014.11.012

DeNardo, D. G., Brennan, D. J., Rexhepaj, E., Ruffell, B., Shiao, S. L., Madden, S. F., . . . Coussens, L. M. (2011). Leukocyte complexity predicts breast cancer survival and functionally regulates response to chemotherapy. *Cancer Discov, 1*(1), 54-67. doi:10.1158/2159-8274.CD-10-0028

Eggert, T., Wolter, K., Ji, J., Ma, C., Yevsa, T., Klotz, S., . . . Greten, T. F. (2016). Distinct Functions of Senescence-Associated Immune Responses in Liver Tumor Surveillance and Tumor Progression. *Cancer Cell, 30*(4), 533-547. doi:10.1016/j.ccell.2016.09.003

Finisguerra, V., Di Conza, G., Di Matteo, M., Serneels, J., Costa, S., Thompson, A. A. R., . . . Mazzone, M. (2015). MET is required for the recruitment of anti-tumoural neutrophils. *Nature, 522*(7556), 349-353. doi:10.1038/nature14407

Forssell, J., Oberg, A., Henriksson, M. L., Stenling, R., Jung, A., & Palmqvist, R. (2007). High macrophage infiltration along the tumor front correlates with improved survival in colon cancer. *Clin Cancer Res, 13*(5), 1472-1479. doi:10.1158/1078-0432.CCR-06-2073

Fossati, G., Ricevuti, G., Edwards, S. W., Walker, C., Dalton, A., & Rossi, M. L. (1999). Neutrophil infiltration into human gliomas. *Acta Neuropathologica, 98*(4), 349-354. doi:10.1007/s004010051093

Franklin, R. A., Liao, W., Sarkar, A., Kim, M. V., Bivona, M. R., Liu, K., . . . Li, M. O. (2014). The cellular and molecular origin of tumor-associated macrophages. *Science, 344*(6186), 921-925. doi:10.1126/science.1252510

Galdiero, M. R., Bonavita, E., Barajon, I., Garlanda, C., Mantovani, A., & Jaillon, S. (2013). Tumor associated macrophages and neutrophils in cancer. *Immunobiology, 218*(11), 1402-1410. doi:10.1016/j.imbio.2013.06.003

Gandhi, L., Camidge, D. R., Ribeiro de Oliveira, M., Bonomi, P., Gandara, D., Khaira, D., . . . Rudin, C. M. (2011). Phase I study of Navitoclax (ABT-263), a novel Bcl-2 family inhibitor, in patients with small-cell lung cancer and other solid tumors. *Journal of clinical oncology : official journal of the American Society of Clinical Oncology, 29*(7), 909-916. doi:10.1200/JCO.2010.31.6208

Gentles, A. J., Newman, A. M., Liu, C. L., Bratman, S. V., Feng, W., Kim, D., . . . Alizadeh, A. A. (2015). The prognostic landscape of genes and infiltrating immune cells across human cancers. *Nat Med, 21*(8), 938-945. doi:10.1038/nm.3909

Giulian, D. (1987). Ameboid microglia as effectors of inflammation in the central nervous system. *Journal of Neuroscience Research, 18*(1), 155-171. doi:10.1002/jnr.490180123

Granot, Z., Henke, E., Comen, E. A., King, T. A., Norton, L., & Benezra, R. (2011). Tumor entrained neutrophils inhibit seeding in the premetastatic lung. *Cancer Cell, 20*(3), 300-314. doi:10.1016/j.ccr.2011.08.012

Hanahan, D., & Weinberg, R. A. (2000). The hallmarks of cancer. *Cell, 100*(1), 57-70.

Hanahan, D., & Weinberg, R. A. (2011). Hallmarks of cancer: the next generation. *Cell, 144*(5), 646-674. doi:10.1016/j.cell.2011.02.013

Hoare, M., & Narita, M. (2013). Transmitting senescence to the cell neighbourhood. *Nat Cell Biol, 15*(8), 887-889. doi:10.1038/ncb2811

Hussain, S. F., Yang, D., Suki, D., Aldape, K., Grimm, E., & Heimberger, A. B. (2006). The role of human glioma-infiltrating microglia/macrophages in mediating antitumor immune responses. *Neuro-oncology, 8*(3), 261-279. doi:10.1215/15228517-2006-008

Kaur, C., Rathnasamy, G., & Ling, E. A. (2017). Biology of Microglia in the Developing Brain. *J Neuropathol Exp Neurol, 76*(9), 736-753. doi:10.1093/jnen/nlx056

Kierdorf, K., Katzmarski, N., Haas, C. A., & Prinz, M. (2013). Bone marrow cell recruitment to the brain in the absence of irradiation or parabiosis bias. *PLoS One, 8*(3), e58544-e58544. doi:10.1371/journal.pone.0058544

Krieg, C., Nowicka, M., Guglietta, S., Schindler, S., Hartmann, F. J., Weber, L. M., . . . Becher, B. (2018). High-dimensional single-cell analysis predicts response to anti-PD-1 immunotherapy. *Nature Medicine, 24*, 144. doi:10.1038/nm.4466

https://www.nature.com/articles/nm.4466#supplementary-information

Kumar, V., Patel, S., Tcyganov, E., & Gabrilovich, D. I. (2016). The Nature of Myeloid-Derived Suppressor Cells in the Tumor Microenvironment. *Trends Immunol, 37*(3), 208-220. doi:10.1016/j.it.2016.01.004

Leblond, M. M., Gerault, A. N., Corroyer-Dulmont, A., MacKenzie, E. T., Petit, E., Bernaudin, M., & Valable, S. (2016). Hypoxia induces macrophage polarization and re-education toward an M2 phenotype in U87 and U251 glioblastoma models. *Oncoimmunology, 5*(1), e1056442. doi:10.1080/2162402X.2015.1056442

Lee, C., Lee, J., Choi, S. A., Kim, S. K., Wang, K. C., Park, S. H., . . . Phi, J. H. (2018). M1 macrophage recruitment correlates with worse outcome in SHH Medulloblastomas. *BMC Cancer, 18*(1), 535. doi:10.1186/s12885-018-4457-8

Leifler, K. S., Svensson, S., Abrahamsson, A., Bendrik, C., Robertson, J., Gauldie, J., . . . Dabrosin, C. (2013). Inflammation induced by MMP-9 enhances tumor regression of experimental breast cancer. *J Immunol, 190*(8), 4420-4430. doi:10.4049/jimmunol.1202610

Lewis, C. E., Harney, A. S., & Pollard, J. W. (2016). The Multifaceted Role of Perivascular Macrophages in Tumors. *Cancer Cell, 30*(1), 18-25. doi:10.1016/j.ccell.2016.05.017

Liang, W., & Ferrara, N. (2016). The Complex Role of Neutrophils in Tumor Angiogenesis and Metastasis. *Cancer Immunol Res, 4*(2), 83-91. doi:10.1158/2326-6066.CIR-15-0313

Louis, D. N., Perry, A., Reifenberger, G., von Deimling, A., Figarella-Branger, D., Cavenee, W. K., . . . Ellison, D. W. (2016). The 2016 World Health Organization Classification of Tumors of the Central Nervous System: a summary. *Acta Neuropathol, 131*(6), 803-820. doi:10.1007/s00401-016-1545-1

Mantovani, A., Sozzani, S., Locati, M., Allavena, P., & Sica, A. (2002). Macrophage polarization: tumor-associated macrophages as a paradigm for polarized M2 mononuclear phagocytes. *Trends in Immunology, 23*(11), 549-555. doi:https://doi.org/10.1016/S1471-4906(02)02302-5

Margol, A. S., Robison, N. J., Gnanachandran, J., Hung, L. T., Kennedy, R. J., Vali, M., . . . Asgharzadeh, S. (2015). Tumor-associated macrophages in SHH subgroup of medulloblastomas. *Clin Cancer Res, 21*(6), 1457-1465. doi:10.1158/1078-0432.CCR-14-1144

Maximov, V., Chen, Z., Wei, Y., Robinson, M. H., Herting, C. J., Shanmugam, N. S., . . . Kenney, A. M. (2019). Tumour-associated macrophages exhibit anti-tumoural properties in Sonic Hedgehog medulloblastoma. *Nature Communications, 10*(1), 2410. doi:10.1038/s41467-019-10458-9

Mehrabi, M., Amini, F., & Mehrabi, S. (2018). Active Role of the Necrotic Zone in Desensitization of Hypoxic Macrophages and Regulation of CSC-Fate: A hypothesis. *Frontiers in Oncology, 8*. doi:10.3389/fonc.2018.00235

Metcalfe, C., & de Sauvage, F. J. (2011). Hedgehog fights back: mechanisms of acquired resistance against Smoothened antagonists. *Cancer Res, 71*(15), 5057-5061. doi:10.1158/0008-5472.CAN-11-0923

Milanovic, M., Fan, D. N. Y., Belenki, D., Dabritz, J. H. M., Zhao, Z., Yu, Y., . . . Schmitt, C. A. (2018). Senescence-associated reprogramming promotes cancer stemness. *Nature, 553*(7686), 96-100. doi:10.1038/nature25167

Mille, F., Tamayo-Orrego, L., Levesque, M., Remke, M., Korshunov, A., Cardin, J., . . . Charron, F. (2014). The Shh receptor Boc promotes progression of early medulloblastoma to advanced tumors. *Dev Cell, 31*(1), 34-47. doi:10.1016/j.devcel.2014.08.010

Morantz, R. A., Wood, G., W. , Foster, M., Clark, M., & Gollahon, K. (1979). Macrophages in experimental and human brain tumors. *Journal of Neurosurgery, 50*(3), 305-311. doi:10.3171/jns.1979.50.3.0305

Mosteiro, L., Pantoja, C., Alcazar, N., Marion, R. M., Chondronasiou, D., Rovira, M., . . . Serrano, M. (2016). Tissue damage and senescence provide critical signals for cellular reprogramming in vivo. *Science, 354*(6315). doi:10.1126/science.aaf4445

Murdoch, C., Muthana, M., Coffelt, S. B., & Lewis, C. E. (2008). The role of myeloid cells in the promotion of tumour angiogenesis. *Nat Rev Cancer, 8*(8), 618-631. doi:10.1038/nrc2444

Murray, P. J., Allen, J. E., Biswas, S. K., Fisher, E. A., Gilroy, D. W., Goerdt, S., . . . Wynn, T. A. (2014). Macrophage activation and polarization: nomenclature and experimental guidelines. *Immunity, 41*(1), 14-20. doi:10.1016/j.immuni.2014.06.008

Northcott, P. A., Jones, D. T., Kool, M., Robinson, G. W., Gilbertson, R. J., Cho, Y. J., . . . Pfister, S. M. (2012). Medulloblastomics: the end of the beginning. *Nat Rev Cancer, 12*(12), 818-834. doi:10.1038/nrc3410

Papavasiliou, A. K., Mehler, M. F., Mabie, P. C., Marmur, R., Qingbin, S., Keating, R. F., & Kessler, J. A. (1997). Paracrine Regulation of Colony-stimulating Factor-1 in Medulloblastoma: Implications for Pathogenesis and Therapeutic Interventions. *Neurosugery, 41*(4), 916-923.

Parkhurst, Christopher N., Yang, G., Ninan, I., Savas, Jeffrey N., Yates, John R., III, Lafaille, Juan J., . . . Gan, W.-B. (2013). Microglia Promote Learning-Dependent Synapse Formation through Brain-Derived Neurotrophic Factor. *Cell, 155*(7), 1596-1609. doi:10.1016/j.cell.2013.11.030

Pham, C. D., Flores, C., Yang, C., Pinheiro, E. M., Yearley, J. H., Sayour, E. J., . . . Mitchell, D. A. (2016). Differential Immune Microenvironments and Response to Immune Checkpoint Blockade among Molecular Subtypes of Murine Medulloblastoma. *Clin Cancer Res, 22*(3), 582-595. doi:10.1158/1078-0432.CCR-15-0713

Phoenix, T. N., Patmore, D. M., Boop, S., Boulos, N., Jacus, M. O., Patel, Y. T., . . . Gilbertson, R. J. (2016). Medulloblastoma Genotype Dictates Blood Brain Barrier Phenotype. *Cancer Cell, 29*(4), 508-522. doi:10.1016/j.ccell.2016.03.002

Powell, D. R., & Huttenlocher, A. (2016). Neutrophils in the Tumor Microenvironment. *Trends Immunol, 37*(1), 41-52. doi:10.1016/j.it.2015.11.008

Priller, J., Flügel, A., Wehner, T., Boentert, M., Haas, C. A., Prinz, M., . . . Dirnagl, U. (2001). Targeting gene-modified hematopoietic cells to the central nervous system: Use of green fluorescent protein uncovers microglial engraftment. *Nature Medicine, 7*(12), 1356-1361. doi:10.1038/nm1201-1356

Pyonteck, S. M., Akkari, L., Schuhmacher, A. J., Bowman, R. L., Sevenich, L., Quail, D. F., . . . Joyce, J. A. (2013). CSF-1R inhibition alters macrophage polarization and blocks glioma progression. *Nat Med, 19*(10), 1264-1272. doi:10.1038/nm.3337

Qian, B. Z., Li, J., Zhang, H., Kitamura, T., Zhang, J., Campion, L. R., . . . Pollard, J. W. (2011). CCL2 recruits inflammatory monocytes to facilitate breast-tumour metastasis. *Nature, 475*(7355), 222-225. doi:10.1038/nature10138

Qian, B. Z., & Pollard, J. W. (2010). Macrophage diversity enhances tumor progression and metastasis. *Cell, 141*(1), 39-51. doi:10.1016/j.cell.2010.03.014

Quail, D. F., & Joyce, J. A. (2017). The Microenvironmental Landscape of Brain Tumors. *Cancer Cell, 31*(3), 326-341. doi:10.1016/j.ccell.2017.02.009

Rhee, I. (2016). Diverse macrophages polarization in tumor microenvironment. *Arch Pharm Res, 39*(11), 1588-1596. doi:10.1007/s12272-016-0820-y

Ries, C. H., Cannarile, M. A., Hoves, S., Benz, J., Wartha, K., Runza, V., . . . Ruttinger, D. (2014). Targeting tumor-associated macrophages with anti-CSF-1R antibody reveals a strategy for cancer therapy. *Cancer Cell, 25*(6), 846-859. doi:10.1016/j.ccr.2014.05.016

Roggendorf, W., Strupp, S., & Paulus, W. (1996). Distribution and characterization of microglia/macrophages in human brain tumors. *Acta Neuropathologica, 92*(3), 288-293. doi:10.1007/s004010050520

Roh-Johnson, M., Shah, A. N., Stonick, J. A., Poudel, K. R., Kargl, J., Yang, G. H., . . . Moens, C. B. (2017). Macrophage-Dependent Cytoplasmic Transfer during Melanoma Invasion In Vivo. *Dev Cell, 43*(5), 549-562 e546. doi:10.1016/j.devcel.2017.11.003

Rossi, M. L., Buller, J. R., Heath, S. A., Carey, M. P., Carboni, P., Koutsoubelis, G., & Coakham, H. B. (1991). The Monocyte/Macrophage Infiltrate in 35 Medulloblastomas: A Paraffin-Wax Study. *Tumori Journal, 77*(1), 36-40. doi:10.1177/030089169107700109

Saleh, T., Tyutynuk-Massey, L., Cudjoe, E. K., Idowu, M. O., Landry, J. W., & Gewirtz, D. A. (2018). Non-Cell Autonomous Effects of the Senescence-Associated Secretory Phenotype in Cancer Therapy. *Frontiers in Oncology, 8*. doi:10.3389/fonc.2018.00164

Salminen, A., Kauppinen, A., & Kaarniranta, K. (2012). Emerging role of NF-κB signaling in the induction of senescence-associated secretory phenotype (SASP). *Cellular Signalling, 24*(4), 835-845. doi:https://doi.org/10.1016/j.cellsig.2011.12.006

Sceneay, J., Chow, M. T., Chen, A., Halse, H. M., Wong, C. S. F., Andrews, D. M., . . . Möller, A. (2012). Primary Tumor Hypoxia Recruits CD11b+/Ly6Cmed/Ly6G+ Immune Suppressor Cells and Compromises NK Cell Cytotoxicity in the Premetastatic Niche. *Cancer Research, 72*(16), 3906. doi:10.1158/0008-5472.CAN-11-3873

Scott, C. L., Zheng, F., De Baetselier, P., Martens, L., Saeys, Y., De Prijck, S., . . . Guilliams, M. (2016). Bone marrow-derived monocytes give rise to self-renewing and fully differentiated Kupffer cells. *Nature Communications, 7*, 10321. doi:10.1038/ncomms10321

https://www.nature.com/articles/ncomms10321#supplementary-information

Sevenich, L. (2018). Brain-Resident Microglia and Blood-Borne Macrophages Orchestrate Central Nervous System Inflammation in Neurodegenerative Disorders and Brain Cancer. *Frontiers in Immunology, 9*, 697.

Tamayo-Orrego, L., Wu, C. L., Bouchard, N., Khedher, A., Swikert, S. M., Remke, M., . . . Charron, F. (2016). Evasion of Cell Senescence Leads to Medulloblastoma Progression. *Cell Rep, 14*(12), 2925-2937. doi:10.1016/j.celrep.2016.02.061

Taylor, M. D., Northcott, P. A., Korshunov, A., Remke, M., Cho, Y. J., Clifford, S. C., . . . Pfister, S. M. (2012). Molecular subgroups of medulloblastoma: the current consensus. *Acta Neuropathol, 123*(4), 465-472. doi:10.1007/s00401-011-0922-z

Wang, M., Zhao, J., Zhang, L., Wei, F., Lian, Y., Wu, Y., . . . Guo, C. (2017). Role of tumor microenvironment in tumorigenesis. *J Cancer, 8*(5), 761-773. doi:10.7150/jca.17648

Wechsler-Reya, R. J., & Scott, M. P. (1999). Control of Neuronal Precursor Proliferation in the Cerebellum by Sonic Hedgehog. *Neuron, 22*(1), 103-114. doi:https://doi.org/10.1016/S0896-6273(00)80682-0

Yauch, R. L., Dijkgraaf, G. J. P., Alicke, B., Januario, T., Ahn, C. P., Holcomb, T., . . . de Sauvage, F. J. (2009). Smoothened Mutation Confers Resistance to a Hedgehog Pathway Inhibitor in Medulloblastoma. *Science, 326*(5952), 572. doi:10.1126/science.1179386

Zhang, Q. W., Liu, L., Gong, C. Y., Shi, H. S., Zeng, Y. H., Wang, X. Z., . . . Wei, Y. Q. (2012). Prognostic significance of tumor-associated macrophages in solid tumor: a meta-analysis of the literature. *PLoS One, 7*(12), e50946. doi:10.1371/journal.pone.0050946

Zhu, Y., Doornebal, E. J., Pirtskhalava, T., Giorgadze, N., Wentworth, M., Fuhrmann-Stroissnigg, H., . . . Kirkland, J. L. (2017). New agents that target senescent cells: the flavone, fisetin, and the BCL-X(L) inhibitors, A1331852 and A1155463. *Aging, 9*(3), 955-963. doi:10.18632/aging.101202

Zhu, Y., Herndon, J. M., Sojka, D. K., Kim, K. W., Knolhoff, B. L., Zuo, C., . . . DeNardo, D. G. (2017). Tissue-Resident Macrophages in Pancreatic Ductal Adenocarcinoma Originate from Embryonic Hematopoiesis and Promote Tumor Progression. *Immunity, 47*(2), 323-338 e326. doi:10.1016/j.immuni.2017.07.014

Zhu, Y., Tchkonia, T., Pirtskhalava, T., Gower, A. C., Ding, H., Giorgadze, N., . . . Kirkland, J. L. (2015). The Achilles' heel of senescent cells: from transcriptome to senolytic drugs. *Aging Cell, 14*(4), 644-658. doi:10.1111/acel.12344